THE RELATIONSHIPS OF PARTICULATE MATTER AND PARTICULATE ORGANIC CARBON WITH HYPOXIC CONDITIONS ALONG THE TEXAS-LOUISIANA SHELF

A Thesis

by

NICOLE A. ZUCK

Submitted to the Office of Graduate and Professional Studies of
Texas A&M University
in partial fulfillment of the requirements for the degree of

MASTER OF SCIENCE

Chair of Committee,	Wilford Gardner
Co-Chair of Committee,	Mary Jo Richardson
Committee Member,	Steven DiMarco
Head of Department,	Deborah Thomas

August 2014

Major Subject: Oceanography

ABSTRACT

The Mississippi-Atchafalaya river system discharges into the northern Gulf of Mexico and peaks during the spring freshet bringing high levels of nutrients that spur eutrophication in surface waters, often resulting in hypoxic (dissolved oxygen concentrations less than 1.4 mL/L) sub-pycnocline conditions. Hypoxia is generally manifest seasonally along the Louisiana coast over the shelf. In summer 2011, high rainfall in the Mississippi-Atchafalaya watershed caused high discharge into the northern Gulf of Mexico. In summer 2012 drought conditions in the watershed significantly reduced the discharge. Summer 2013 conditions returned to the climatologic average river discharge. Discrete samples were collected and continuous measurements were made via an onboard surface-water flow-through system, CTD casts, and by an undulating towed vehicle. Total particulate matter and particulate organic carbon samples were obtained from Niskin bottles on CTD casts. Samples were also taken to measure dissolved oxygen concentration and nutrients along with other hydrographic parameters. Water-column particulate matter and particulate organic carbon were analyzed to investigate the relationship between hypoxia and the composition of the particulate matter along the Texas-Louisiana shelf during different discharge rates in summer 2011 (for C:N of particulate matter), 2012 and 2013 for a larger suite of particle composition and relationship to hydrographic conditions of the Mississippi-Atchafalaya river system. The goal of this research is to determine if a statistically significant relationship is manifest, between shelf hypoxia and total particulate matter, as well as

between particulate organic carbon and hypoxia, during periods of different river discharge (i.e. average, flood, or drought conditions). Correlations were identified between some variables, but no direct relationship between particulate matter and hypoxia was observed. There were however, some statistically significant changes in several parameters between summer 2013 and summer 2013.

ACKNOWLEDGEMENTS

I would like to thank my committee chair and co-chair, Dr. Gardner and Dr. Richardson, and my committee member, Dr. DiMarco, for their guidance and support throughout the course of this research.

Much appreciation and thanks to my colleagues, department faculty and staff, for their support and encouragement throughout the course of this research. They have truly made my time here at Texas A&M University a fantastic and memorable experience.

I would also like to thank the Virginia Institute of Marine Science, especially Erin Ferer in Dr. Elizabeth Canuel's laboratory, who performed my sample analysis for POC. Thanks must also be extended to the National Science Foundation (NSF 0806926) and Earl F. Cook Professorship to Dr. Gardner, and to the Department of Oceanography for funding me in my research.

Finally, I cannot thank my family and friends enough for their encouragement and love throughout this process. They are truly my motivation.

TABLE OF CONTENTS

LIST OF FIGURES

LIST OF TABLES

1. INTRODUCTION

Hypoxia (low oxygen conditions) in bottom coastal waters, commonly known as dead zones, has spread exponentially in the last 50 years [*Diaz and Rosenberg*, 2011; *Diaz and Rosenberg*, 2008]. Hypoxia historically has been a natural phenomenon, but the recent increase in hypoxic areas is largely due to industrial and agricultural growth, especially with the increased use of manufactured fertilizers [*Rabalais et al*., 2014]. Hypoxia is often exacerbated by extreme surface water productivity, driven by eutrophication caused by fertilizers in river runoff. This surface productivity enhances the export of organic matter and detritus to the sediments, fueling microbial respiration and depriving bottom waters of dissolved oxygen. As of 2008, dead zones have impacted over 245,000 square kilometers [*Diaz and Rosenberg*, 2008] through several ecosystems across the world.

This issue is of particular importance along the Texas-Louisiana shelf in the northern Gulf of Mexico, where the fishing and shrimp industry is a mainstay of many coastal economies [*O'Connor and Whitall*, 2007; *Diaz and Rosenberg*, 2011]. When the concentration of dissolved oxygen begins to decline in bottom waters, most species of fish are able to move away from the afflicted area. Many benthic species, however, are less mobile and may become stressed and eventually perish [*Rabalais et al.*, 2010].

The point at which low oxygen concentration negatively affects marine life varies by species, thus it varies regionally by the dominant species present [*Rabalais et al.*, 2010; *Diaz et al*. 2009]. There is no universal convention on what concentration of dissolved oxygen constitutes hypoxia, but rather regional agreement on the hypoxic

threshold for that area [*Rabalais et al.*, 2010]. In the northern Gulf of Mexico, the experimentally determined tolerance of brown shrimp to low oxygen conditions [*O'Connor and Whitall*, 2007] has been used to establish the hypoxic threshold for the region [*Rabalais et al.*, 2010].

1.1 Spatial and Temporal Setting

Bottom-water hypoxia along the Texas-Louisiana shelf, particularly along the coast of Louisiana, has been studied annually from spring through summer since mid-1980s. The operational definition of hypoxia in the northern Gulf of Mexico is dissolved oxygen concentration in seawater less than 2 mg/L, or less than 1.4mL/L [*Diaz*, 2001]. These conditions typically occur in bottom waters [*Rabalais et al.*, 2010; *Rowe and Chapman*, 2002]. Along the Texas-Louisiana shelf, hypoxia is generally the result of nutrient-loaded freshwater input from the Mississippi-Atchafalaya River system, fueled by eutrophication in surface waters [*Rabalais et al.*, 2010] and isolated by strong stratification. The stratification is intensified by the seasonal change in wind direction, prohibiting mixing [*Hetland and DiMarco*, 2008; *Bianchi et al.*, 2010a].

The Mississippi-Atchafalaya river watershed covers approximately 41% of North America [*Rossi et al.*, 2009], draining the region between the Rocky Mountains to the west and the Appalachian Mountains to the east. The Mississippi drainage basin is so large that it is divided into six sub-basins (Figure 1). The amount of nutrient runoff from pollution, farming, and land erosion entering the rivers has increased since the 1950's [*Rabalais et al.*, 2002]. Currently, it is estimated that between 1.2 million metric tons of

nitrogen and 0.15 million metric tons of phosphorous enter the northern Gulf of Mexico annually via the Mississippi and Atchafalaya rivers [*Bianchi at al.*, 2010b]. Studies indicate that the nitrogen levels have decreased since the last maximum in 1990, however both nitrogen and phosphorous input has remained stable since 1995 [*Turner et al.*, 2007; *Bianchi et al.,* 2010b]. The influx of excess nutrients, particularly nitrogen, begins with the spring freshet and continues through summer, fueling eutrophication in surface waters [*Quigg et al.*, 2011]. Spring/summer eutrophication in surface waters produces organic matter that settles to deeper waters, thus increasing the oxygen demand in bottom waters via microbial respiration, creating hypoxia in the bottom water (Figure 2). Although the extent of the annual hypoxic area varies, the northern Gulf of Mexico experiences on average a total hypoxic area greater than 13,600km^2 [*Dale et al.*, 2010].

The hypoxic region is manifest primarily along the Louisiana coast between the mouths of the Mississippi and Atchafalaya Rivers [*Bianchi et al.*, 2008]. The study area along the Texas-Louisiana shelf is from south of Galveston Bay to the Mississippi River delta. Figure 3 displays all sample locations, plotted on a map of bottom dissolved oxygen concentrations averaged from 2000 to 2007 [*DiMarco,* unpublished]. These station locations are representative of the area sampled annually during June and August, and are repeated each year, weather and sea condition permitting. During periods of severe hypoxia, some additional stations were added to help quantify the extent of the hypoxic areas. The cruise maps showing sampling locations and Acrobat (a towed undulating vehicle) line locations for June 2012, August 2012, June 2013, and August 2013, are displayed in Figures 4-7. Note that all cruises contain Acrobat lines between

96°W and 88°W, except for August 2013 where the easternmost extent was 90°W due to rough seas. That area was sampled only with the CTD rosette, not the Acrobat.

Hypoxia is a seasonal phenomenon that is recurrent in nature [*Rabalais et al.*, 2010]. It typically occurs during summer months, and manifests in patches over a large area. The hypoxic patches can form in a matter of days, and may persist for days to weeks [*Bianchi et al.*, 2010; *Rabalais et al.*, 2010]. However, dissolved oxygen concentrations may not need to change drastically in order to cross the operational boundary between hypoxic and non-hypoxic. For example, during summer 2011 the calculated area of hypoxia was very similar for both June and August (Figure 8); however, June displays much lower overall dissolved oxygen concentrations with values just above the hypoxia threshold, whereas August has much larger areas of oxygenated water [*Cochran*, 2013].

1.2 Mechanisms Controlling Hypoxia

Hypoxia along the Texas-Louisiana shelf is a highly complex problem, the extent of which is determined by various factors in addition to seasonal eutrophication. This includes physical factors such as river discharge and wind-forcing [*Feng et al.*, 2012; *Forrest et al*, 2011], as well as the varying flux of sediments and nutrients in three characteristic zones of water along the shelf, defined by *Rowe and Chapman* [2002] and refined by *Bianchi et al.* [2010a] and *Dale et al.* [2010]. These zones, referred to as 'blue,' 'green,' and 'brown' waters [*Rowe and Chapman*, 2002], are determined by turbidity, stratification, and productivity, which together alter the mechanisms driving

hypoxia. It should be noted, however, that each zone is defined by the dominance of specific processes, not a specific geographic location. The areal extent of each zone varies considerably, both seasonally and spatially due to driving forces that create hypoxia.

Within the river plumes, high surface particle concentration limits primary production by preventing light penetration into the lower water column. This area is referred to as the 'brown' zone due to the high particle concentrations present. Organic matter reaching bottom waters or deposited on the seafloor is broken down by microbial respiration, consuming dissolved oxygen [*Diaz*, 2001]. Water-column stratification here is strong due to the buoyant river plume and prevents oxygenated surface water mixing with sub-pycnocline waters.

The next zone is further from the riverine sources of high inorganic sediment input, and primary production dominates. This zone is referred to as the 'green' zone, due to the characteristic abundance of surface-water photosynthesizers. There is sufficient light penetration in surface waters for primary production in this zone because much of the particulate matter has aggregated and settled out or consumed and removed [*Dagg and Breed*, 2003; *Dagg et al.*, 2004]. It is in this zone that the general hypoxia model applies; eutrophication from nutrient input fuels surface production, organic matter settles through stratified waters, and microbial respiration in bottom waters and on the seafloor depletes bottom waters of oxygen (refer to Figure 2).

The third zone considered here is characterized by extremely low nutrient concentrations that result in minimal surface productivity and moderate stratification.

This zone is referred to as the 'blue' zone, due to the water's blue appearance resulting from minimal turbidity from either riverine particles or phytoplankton production. Due to the low-salinity surface waters, stratification is still sufficiently strong to prohibit oxygenated surface waters from mixing with sub-pycnocline waters [*Rowe and Chapman*, 2002], sometimes creating hypoxic conditions. Sub-pycnocline primary production may occur in this zone consuming regenerated nitrogen in summer [*Schaeffer et al.*, 2012; *Cochran*, 2013]; however, net respiration dominates in these bottom waters.

1.3 Objectives and Hypotheses

The main objective of this work is to examine the relationship between hypoxia and the concentration and bulk composition of the particulate matter along the Texas-Louisiana shelf during different discharge rates of the Mississippi-Atchafalaya river system. Summer 2011 is characterized by high river discharge due to flooding in the upper Mississippi River basin, whereas summer 2012 and summer 2013, represent a drought year and an average discharge year, respectively (Figure 9). To assess a relationship between particulates and hypoxia, the objective of this research consists of four scientific hypotheses (H1, H2, H3 and H4):

H1) The 2012 low runoff conditions result in lower PM concentrations, lower percent and concentration of POC, and higher C:N along the shelf than during the 2013 average runoff conditions.

H2) POC, as well as PM are impacted by and impact hypoxic conditions in the northern Gulf of Mexico.

H3) Biomass, as well as resuspended sediments are impacted by and impact hypoxic conditions in the northern Gulf of Mexico.

H4) The 2011 high runoff conditions due to flooding in the upper Mississippi river basin result in significant seasonal differences in carbon isotopic ranges and in the isotopic C:N ratio in the PM, whereas nitrogen isotope ranges remain the same.

Linear regressions models are used to the "goodness of fit" of the relationship between two parameters using the coefficient of determination, R^2. The Wilcoxin Rank-Sum test is used to test the hypotheses where the data have skewed distributions. This test is designed to statically determine if two skewed data sets are essentially the same, or if they are significantly different from each other. H1 and H4 are tested using the Wilcoxin Rank-Sum test.

To test H1 regarding the potential difference in particle properties seasonally and inter-annually, the concentration of total particulate matter (PM) and percentage and concentration of particulate organic carbon (POC), and the C:N ratio are used in regressions with oxygen concentration, longitude, and depth. A null hypothesis holds if there is lower PM, POC, and higher C:N in 2012 than 2013.

To test H2 regarding POC, as well as PM being impacted by and impacting hypoxic conditions linear regressions between PM, POC and oxygen concentration both along shelf and within the water column at nominal depths (surface, middle, and bottom) are used. Sub-regions along the shelf were analyzed to identify correlations between variables on smaller spatial scales. A null hypothesis holds when there is a high degree of randomness as indicated by low (< 0.4) R^2 values.

To test H3 regarding biomass, as well as resuspended sediments being impacted by and impacting hypoxic conditions linear regressions of b_b (a proxy for PM) vs O_2 in sub-pycnocline hypoxic waters, chl-*a* fluorescence (as a proxy for biomass) vs. O_2 in sub-pycnocline hypoxic waters and b_b vs. chl-*a* fluorescence in sub-pycnocline hypoxic waters, are tested in different regions dependent of the dominant processes. This hypothesis is tested using values of R^2 in different zones ('brown,' 'green,' 'blue'). A null hypothesis holds when R^2 values are low (< 0.4) indicating minimal correlation between variables.

H4 tests whether statistically significant seasonal variations in the stable C and N isotopic composition of the particulate matter exist. The concentration of the $PO^{13}C$ and $PO^{15}N$ components of the PM are used to indicate seasonal changes in isotopic composition of PM. This hypothesis is tested statistically using the Wilcoxin Rank-Sum test.

2. METHODS

2.1 *Sample Collection*

Continuous measurements and discrete samples were collected in three basic ways; shipboard surface-water flow-through system in the shipboard wet lab, CTD casts, and a Sea Sciences Inc. Acrobat undulating towed vehicle (Acrobat). These methods are discussed below. See Table 1 for a summary of all equipment and related samples.

A rosette containing six 4-L Niskin bottles, CTD, WetLabs FLNTU (chlorophyll-*a* fluorescence and backscatter), and dissolved oxygen probe, was deployed to make continuous profiles through the water column as well as collect samples from three nominal depths, bottom (within 1 meter), middle, and surface (upper 1 meter) of the water column (Table 1). The water depth in the study area varied across and along the shelf from approximately 5 to 51m. Total particulate matter (PM) samples were drawn from the Niskin bottles into 0.5L bottles. Particulate organic carbon (POC) samples were drawn into opaque 1.0L bottles. On a few casts, containers were used to collect the water remaining in the Niskin bottle below the spigot to test for the collection of rapidly settling particles (dregs) [*Gardner et al.*, 2001]. All sample bottles were stored out of sunlight until they were filtered onboard.

PM and dregs samples were vacuum filtered through Poretics 47.0mm polycarbonate membrane filters with a 0.4μm pore size (PM filters). The filters were catalogued and stored in 50.0mm plastic petri dishes with lids. The POC samples were vacuum filtered through Whatman 25mm glass microfiber filters (GF/F). The GF/F filters were then individually wrapped in aluminum foil, labeled, and frozen until they

could be processed. The volume of water filtered was measured with a graduated cylinder for all samples.

Onboard surface flow-through measurements, including temperature, salinity, colored dissolved organic matter (CDOM fluorescence), beam transmission and chlorophyll fluorescence were also collected (Table 1). The Acrobat was towed in lines perpendicular to the coast; however, weather conditions occasionally necessitated a change in tow direction, or the cancellation of a line. Most notably, during August 2012 (Figure 5) there are two Acrobat lines that run parallel to the coast. The Acrobat lines were used to create vertical sections of various properties including salinity, CDOM, dissolved oxygen concentration, fluorescence and turbidity (Table 1). The Acrobat undulated from 1-2 meters below the surface, to 1-2 meters above the bottom, allowing for high vertical and horizontal resolution of approximately 200 meters along each transect path [*DiMarco*, 2013; *Cochran*, 2013].

2.2 *Cruise Preparation and Lab Analysis*

The GF/F filters were pre-combusted in a muffle furnace between approximately 450°C and 650°C for 4 to 6 hours. They were then stored in airtight petri dishes until used for sample filtration. After sample collection, the POC filters were dried for 4 to 6 hours at approximately 40°C to 65°C. The filters were then fumigated in a desiccator containing hydrochloric acid for 24 hours to remove calcium carbonate. After fumigation, they were dried again for 4 to 6 hours. After drying, each filter was wrapped in 30mm tin disks, catalogued, and stored in a 96-well-plate sample holder.

Measurements of particulate organic matter were made on the 2012 and 2013 samples at the Virginia Institute of Marine Science lab using an Eager CHN elemental analyzer. This analysis determined mass of POC and PON, as well as the %C and %N in each sample. The 2011 samples were analyzed at TAMU for stable isotopes in addition to %C and %N.

PM filters were weighed before use to determine a base weight before filtration. After filtration, rinsing 3 times with filtered RO water and drying, they were reweighed to obtain the weight of sediment filtered.

2.3 *Data Analysis*

Concentration of particles in PM is calculated from the measured sediment weight and volume filtered. POC concentration is calculated in a similar manner; however the weights of POC are determined with an Eager CHN. Dregs samples are used to determine the amount of particulate matter lost due to particle settling within the Niskin bottles. The dregs samples collected during the 2012 cruises indicate that the amount of material lost in 15 samples collected was between 3% and 10% in 14 samples and 25% in one sample, which is much smaller than in most deep water sampling where sample extraction may be 3-4 hours after bottles were closed at depth, allowing extended time for settling within the bottle [*Gardner*, 1977]. In this study, time from bottle closure to water extraction was on the order of minutes. The added time and effort for sampling dregs was not deemed worth the small potential difference in bulk concentrations,

therefore no correction factor was applied to the data sets. Once concentrations of PM and POC are determined, the percent of PM that is POC is calculated.

2.3.1 *Optical Measurements*

PM concentrations, and POC concentrations in waters, can be determined with beam attenuation (c_p) or backscatter (b_b) using a transmissometer or backscatter instrument that has been calibrated with simultaneously collected field and/or lab samples [*Gardner et al.*, 2001; *Cetinic et al,*. 2012]. A WetLabs FLNTU backscatter instrument on the rosette yielded data in NTU (normalized turbidity unit) voltage. This was converted to NTU units by

$$\text{NTU} = \text{Scale Factor} \times (\text{Output} - \text{Dark Counts}),$$

and then converted to backscatter (b_b),

$$b_b = 0.0025 \times \text{NTU}$$

[*Ian Walsh, WetLabs*, personal communication].

There is variability in composition of particulate matter through the water column, so different correlations of PM/b_b or POC/b_b may exist in different depth intervals (surface mixed layer, mid-water, and bottom mixed layer) [*Cochran*, 2013]. Calibrations were made both in the field for the three nominal depths- surface, middle, and bottom. Lab calibrations were made using incremental additions of shelf sediment less than 8μm in diameter to water in a dark, enclosed chamber. This controlled test with sediment of uniform particle size and composition displayed a highly linear optical response to particle mass (Figure 10). The field calibration used the PM concentration

determined from the filtered mass weight, plotted against the backscatter measured at the collection depth with samples divided into the three nominal depths (Figures 11 – 14). Chlorophyll-*a* fluorescence sometimes shows a positive correlation with POC concentration in surface waters away from rivers [*Gardner et al.*, 2001; *Holser*, 2011]. It should be noted that the FLNTU on the CTD rosette was moved to the interior of the rosette between 2011 and 2012 to better protect the instrument. The shift caused higher minimum backscatter values (approximately $5b_b \times 10^{-3}$) due to increased reflection from the metal cage (based on air calibrations in a dark lab). After the 2012 cruises, black neoprene rubber was added to the cage inside the rosette, reducing the amount of reflection, and resulting in minimum measurements closer to $0b_b \times 10^{-3}$.

Linear regressions are used to identify correlations between measured parameters such as PM, POC, beam attenuation, C:N, and fluorescence. The C:N also helps decipher between fresh and older, resuspended organic matter, as fresh organic matter from primary production should have a C:N close to 7 [*Redfield et al.*, 1963; *Wissel et al.*, 2005], whereas detritus, and sediment have a much higher C:N [*Wissel et al.*, 2005]. To aid in analysis, surface inline measurements for temperature, salinity, CDOM, and beam attenuation were plotted vs. distance along the shelf to aid in defining brown, green and blue zones (data not shown). Ocean Data View (ODV) is used for mapping all parameters in relation to the Texas-Louisiana Shelf, both at the surface and at desired depths. Cross-shelf sections are plotted from both CTD casts and Acrobat tows using ODV. CTD casts are also used to plot along-shelf sections of all measured parameters,

as well as plot profiles of the water column at each sample station. Statistical analyses are used along with these plots to accept or reject a null hypothesis.

3. RESULTS

In general, both surface and bottom PM concentrations are higher in June than August for both 2012 and 2013, with a lower and narrower concentration range in the middle water column. Hypoxia exists at some part of every Acrobat line in June 2013 (Figure 6), but only exists south of the Mississippi Delta (Lines 15-16; the two lines east of 90°W) in June 2012 (Figure 4). This extreme change in hypoxic conditions is likely attributable to the Mississippi-Atchafalaya River System returning to average flow conditions in 2013, as well as greater wave-induced mixing during cruises in 2012 due to rough seas, allowing oxygen to reach sub-pycnocline waters in shallow areas. Several Acrobat lines and their accompanying CTD casts display this well-mixed water column and oxygenated bottom waters. Examples of such lines are the two between 92°W and 94°W during August 2012 (Figure 15) that run parallel to the coast, and all lines west of 94°W during June 2012.

The middle shelf during August 2012 is very well mixed due to rough water conditions; however stratification can become reestablished in order of days to weeks after the seas settle depending on discharge and winds [*Bianchi et al.*, 2010a]. All cruise tracks away from the river are in the 'green' (Figure 16) and 'blue' (Figure 17) zones. No true 'brown' waters are observed in any cruise tracks. The areas observed with high PM concentrations (> 10 mg/L) are high compared to average shelf concentrations (0-5 mg/L), both at the surface and sub-pycnocline, but are still well below the average concentration of suspended sediment load carried by the Mississippi river (442mg/L or 67.5×10^6 tons/Y) [*Rossi et al.*, 2009; *Mead et al.*, 2012]. The river-derived sediment

rapidly flocculates and settles as the river empties into the Gulf of Mexico, and none of the cruise tracks go close enough to the river mouth to observe this phenomenon.

3.1 *Sub-Pycnocline Productivity and Light Limitation; West of 90°*

During each cruise, we observed areas of high concentrations of chlorophyll-*a* that suggest an abundance of biomass that coincided with, and may be primarily responsible for, the elevated bottom turbidity in some areas. These areas are generally part of the 'blue' zone furthest from the river mouth. These regions are generally towards the western end of our study area, where surface waters are clear enough that light can penetrate to the seafloor allowing deep-water and benthic algal growth [*Schaffer et al.*, 2011]. There are also some areas where high turbidity prohibits light penetration to bottom waters, prohibiting algal growth. This light limitation may be caused by surface phytoplankton blocking light, or by resuspension of sediment near the seafloor, blocking the light. To compare these features between years and seasons, Acrobat lines were selected from the western end, 94°-96° W, and from further east, 90°-92°W, as "representative" sections. Along some sections, the complexity exhibited is beyond the testing of the hypotheses for this work.

3.1.1 *June 2012*

Sub-pycnocline chlorophyll-*a* is apparent between 90°-92° W, and still exists west of 92° but it is not as prevalent. High sub-pycnocline chlorophyll-*a* is particularly obvious south of East Cote Blanche and Atchafalaya Bays in line L11 (Figure 18). Here,

the high chlorophyll-*a* fluorescence near the seafloor, correlates positively and strongly with turbidity, optically measured as backscatter. This is also observed south of Galveston in Line L03 (Figure 19). East of 90° W, high chlorophyll is almost exclusively found at the surface. In line L04 (Figure 20), also south of Galveston, there is resuspension of sediments increasing bottom turbidity, in addition to an increase in fluorescence at or near the seafloor. The close proximity of line L04 to L03 exemplifies how quickly mechanisms can change along the Texas-Louisiana shelf.

3.1.2 *August 2012*

Line L10 (Figure 21), south of East Cote Blanche Bay displays high sub-pycnocline chlorophyll fluorescence, and as seen in June 2012 (Figure 18), there is a positive correlation between turbidity and chlorophyll-*a*. In the west, Line L2 (Figure22) south of Galveston shows a strong positive correlation between bottom turbidity and chlorophyll-*a*. During August, line L3 (Figure 23), also south of Galveston, which had high bottom fluorescence in June (Figure 19), now shows high bottom turbidity with only a small increase with chlorophyll fluorescence in bottom waters. The resuspended sediment may be sufficient to block light and diminish productivity. However, like Line L04 in June 2012 (Figure 20), Line L04 in August 2012 (Figure 24) still displays high turbidity and low sub-pycnocline chlorophyll fluorescence.

3.1.3 *June 2013*

June 2013, unlike the previous year of low discharge, has minimal sub-pycnocline chlorophyll fluorescence in the east. Line L11 (Figure 25) south of East Cote Blanche and Atchafalaya Bays displays high bottom turbidity from resuspension, and a mid-water chlorophyll maximum. This is a stark difference from both June and August of 2012 where there was clear evidence of sub-pycnocline chlorophyll fluorescence. In the west, line L01 (Figure 26) approximates the sub-pycnocline chlorophyll fluorescence and turbidity trend observed in 2012. This line displays much higher chlorophyll-a concentrations (almost 20mg/m^3 here) compared to concentrations less than 4mg/m^3 observed in 2012. This line is also noteworthy in that it displays hypoxic conditions and high CDOM concentration in bottom waters (not shown), despite the high chlorophyll fluorescence likely from *in situ* production. Also observed in June 2013 in Line L14 (Figure 27) southwest of the Mississippi delta; is high bottom water turbidity that is not associated with bottom chlorophyll or the surface water chlorophyll-*a* florescence. The surface chlorophyll, in addition to resuspension creating high turbidity in bottom waters, may be sufficient to block light preventing bottom productivity.

3.1.4 *August 2013*

During August 2013, there is more sub-pycnocline chlorophyll fluorescence than during June 2013; however, sub-pycnocline chlorophyll fluorescence during 2012 is still much more wide spread. Line L022 (Figure 28) south of Galveston displays slightly elevated bottom turbidity, and an increase in chlorophyll fluorescence. In the East, the

portion of line L11 north of 28.7°N (Figure 29) displays both increased bottom chlorophyll and bottom turbidity. This line is important in that south of 28.7°N (Figure 30), the chlorophyll maximum, although associated with increased backscatter, is located above the backscatter maximum. The increased bottom turbidity is likely due to resuspension, and appears to preclude light to the point that primary production cannot occur in the bottom few meters. Profiles in the accompanying CTD cast, Cast L112 (Figure 31), clearly show the turbidity increase below the chlorophyll maximum. In this profile it is also evident that the hypoxic conditions are associated with the chlorophyll maximum as oxygen rapidly decreases at the depth where fluorescence reaches its maximum (~18-24m). Although it may seem counter to the assumption that if increased chlorophyll fluorescence indicates in situ primary production, it should increase oxygen concentrations, the decrease in dissolved oxygen is likely due to net respiration being higher than net production. Elevated chlorophyll fluorescence in low oxygen waters also suggests that primary production can occur in hypoxic waters, as expected.

3.2 *Extension of Low Oxygen Waters Between 88-90°W*

A feature that appears regularly in the Acrobat sections is a pocket of hypoxic waters that forms near the Mississippi River mouth and extends laterally as the seafloor drops steeply. It is very apparent during August 2012 and June 2013 in Line 16 (Figures 32 and 33, respectively), the easternmost repeated Acrobat tow line just south of the Mississippi River delta. During August 2012, additional lines (Figures 34 and 35) were towed at the Mississippi River mouth (Figure 5), giving more detailed structure to the

low oxygen feature. During June 2012, the low oxygen feature is also present near the river mouth, however it was not hypoxic at the time surveyed. This region was not surveyed via Acrobat tow during August 2012; however it is likely that the feature was present, as it existed in the previous three sampling periods.

4. DISCUSSION

4.1 *Hypotheses*

4.1.1 *Hypothesis 1*

The 2012 low runoff conditions are associated with lower PM concentrations, lower percent and concentration of POC, and higher C:N along the shelf than during the 2013 average runoff conditions.

Significant changes in discharge are observed both seasonally and inter-annually. According to calculations done by *Cochran* [2013], it takes approximately 3.2 days for the water to travel from the monitoring gauge at Baton Rouge to the river mouth under average flow conditions, and the effect of the changes in discharge decreases with distance from the river mouth. Other factors influencing the impact of changing river discharge include wind forcing, sea state, and other currents [*Hetland and DiMarco*, 2008]. Incorporating these variables is beyond the scope of this work. The changes in discharge during the study period (Figure 9) are summarized in Table 2, displaying the flow data from May through August of each year, and the magnitude and direction of flow change seasonally and between spring and summer 2012 and 2013 are summarized in Table 3.

Values for PM, POC, %POC and C:N were obtained from bottle samples taken during four cruises along and across the shelf between 96°W to 88°W and return (refer to Figures 4-7). The bottle data sets from each cruise contain between 28 and 45 samples. The distributions are skewed with some very high values that are outliers, but are good data. Since the data have highly skewed distributions, testing the hypothesis

requires a statistical test that can be used on non-normal distributions with different variances in the distributions. The Wilcoxin Rank-Sum test is a useful statistical test for non-normal distributions.

The Wilcoxin Rank-Sum test is based on the rank order of the observations and not the specific values of the observations. It is used as an alternate to the two-sample *t*-test when data are not normally distribution as is the case with these highly skewed data. The Wilcoxin Rank-Sum is used to test the hypotheses that concentrations of PM and POC, percent of POC (%POC) and the C:N ratios of the samples are different between the "low flow" year of 2012 and a "normal" flow year of 2013. Comparisons were made June 2012 to June 2013 and August 2012 to August 2013 (inter-annual) and June 2012 to August 2012 and June 2013 to August 2013 data (seasonal). The P-values indicate the probability that the null hypothesis is rejected or it cannot be rejected at a given confidence level. A 5% confidence level was chosen for the data herein. When the null hypothesis is not rejected the data sets are deemed the same with no significant statistical difference. A rejected null hypothesis indicates that the data sets are significantly different. The results of which are summarized in Table 4.

Another statistical method is to transform the skewed data to a "normal" distribution (Figure 36). A traditional two-tailed *t*-test was run on multiple data sets where the null hypothesis was rejected. The *t*-tests were run with the assumption that the variances of the distributions were the same and the more likely case that the variances of the transformed distributions are different. These tests gave the same results as the Wilcoxin Rank-Sum test, only with higher confidence level and very low p-values.

4.1.1.1 *Particulate Matter*

The PM concentrations were expected to be positively correlated with river discharge; therefore, PM was expected to be higher in June than August of the same year due to the spring freshet increasing the seasonal discharge. River discharge was higher overall during 2013 than in 2012, thus the PM was expected to be greater in 2013.

There is a seasonal distinction between the PM from June to August 2013, both at the surface and at depth. During the 2012 drought, there is no statistical difference between seasons, which may be due to the extremely low discharge. There is also a significant inter-annual increase between June 2012 and June 2013 in both surface and bottom waters. No difference is observed between August 2012 and August 2013 (Table 4).

4.1.1.2 *Particulate Organic Carbon*

Organic matter production decreases from the spring bloom through the summer. Decreased river discharge during the 2012 drought conditions supplied fewer nutrients to the shelf resulting in lower organic matter production. There are significant seasonal differences in surface POC during both years. During 2012, the seasonal difference was observed though the entire water column, whereas 2013 only showed a significant seasonal difference in the surface waters. During both years, the POC is higher in June than August in the surface waters, as is to be expected. There are also inter-annual differences in surface waters between both June 2012 and June 2013, and between August 2012 and 2013 (Table 4).

4.1.1.3 *Percent Particulate Organic Carbon*

Periods of more abundant POC in spring result in higher %POC values than in summer. Also the low discharge year of 2012 has lower POC values and lower % POC. Most POC is derived from marine primary production, so the %POC should be higher seasonally in June, following the spring bloom, than in August, and higher in 2013 than in 2012 due to increased nutrients from higher river discharge. However, contrary to expectations, the %POC was not significantly different seasonally or inter-annually. The only occurrence where the %POC difference was significant was the seasonal difference between June 2012 and August 2012 in the middle of the water column (Table 4).

4.1.1.4 *C:N Ratio*

A POC Redfield Ratio (C:N) of 6.6 indicates that 100% of particulate carbon is plankton [*Wissel et.al.*, 2005], whereas a higher C:N ratio generally indicates older, decaying organic carbon. During June, high river discharge continues following the spring freshet, sustaining a large plankton bloom, resulting in a lower C:N ratio than observed in August when river discharge decreases and organic material has decayed. This hypothesis (H1) is supported by the Wilcoxin Rank-Sum test (Table 4) in all except for surface waters in two cases; seasonally between June 2012 and August 2012, and inter-annually between August 2012 and August 2013. Although Wilcoxin shows a statistical difference, the actual C:N values are low (~ 8). However, it is difficult to identify the processes responsible.

4.1.2 *Hypothesis 2*

POC, as well as PM are impacted by and impact hypoxic conditions in the northern Gulf of Mexico.

The bottle data (Table 5) shows no statistically significant correlations between PM and low dissolved oxygen concentration (< 2mL/L; note hypoxic threshold is 1.4mL/L), or POC and dissolved oxygen at any depths. The bottle data were sorted by the nominal sample depth. In both August 2012 and 2013, a weak correlation between PM and hypoxia is observed. It is seen in bottom waters during August 2012, and in the middle water column during August 2013, however these correlations are not strong. A strong correlation is observed in the middle water column between PM and hypoxia during June 2012, and again between POC and hypoxia during August 2012 (Table 5); however, these strong correlations are based on three data points each and therefore there is little confidence behind the correlations. Only correlations between low oxygen concentration and PM or POC were used, because when using all oxygen values the scatter is extreme and plots as a 'shotgun' pattern.

The Acrobat data is in agreement with the bottle data, showing no strong correlation between backscatter and low dissolved oxygen concentration anywhere during the four cruises. The Acrobat data for this hypothesis were examined regionally in 2° longitude zones. These zones were 88°-90°W, 90°-92°W, 92°-94°W, and 94°-96°W. In the surface 2m of the water column measurements are often noisy due to bubbles generated by the water jet propulsion of the ship, so measurements shallower than 2m are removed. Furthermore, surface waters are always well oxygenated. During

June 2012, there are weak correlations between low O_2 in waters (< 2mL/L) and backscatter between 90°-92°W and 94°-96°W longitudes (Table 5). There are also weak correlations during June 2013 between 94°-96°W and again during August 2013 in the same longitude range. More data are needed to determine if the correlation between backscatter and low O_2 in waters (< 2mL/L) at the far west end of the cruise track is a consistent feature that occurs during August, or an anomaly in the data sets.

4.1.3 *Hypothesis 3*

Biomass, as well as resuspended sediments are impacted by and impact hypoxic conditions in the northern Gulf of Mexico, at least in some areas.

To test this hypothesis only sample data from 10m and deeper in the water column were used. Shallower than 10m, it is difficult to determine whether surface turbidity results from primary production or resuspension and full water column mixing of seafloor sediment. Shallow waters are also likely well mixed and oxygenated; therefore there would be no hypoxia. The data for this hypothesis were also examined regionally in 2° longitude zones. These zones were 88°-90°W, 90°-92°W, 92°-94°W, and 94°-96°W. The data used are summarized in Table 6. It should also be noted that there are no data for the 88°W-90°W longitude region during August 2013.

Overall, there are no statistically significant correlations between biomass, using chlorophyll-*a* concentration as a proxy, and O_2 in hypoxic waters for any of the longitude zones, nor are there any significant correlations between backscatter and hypoxia. There is a small positive correlation (R^2 is 0.4230) between backscatter and

chlorophyll-*a* during June 2013 nearest the river mouth, but this is not observed in any other longitude zone or during summer 2012. In August 2013 this portion of the shelf was not surveyed. There was very little hypoxia observed during summer 2012, and there were no correlations between any of the observed variables in the longitude zones experiencing hypoxic conditions.

At the finer resolution of observing individual Acrobat lines that experienced hypoxia, there are some positive correlations between the observed variables. The data are summarized in Table 7. The correlations observed are not consistent in space or time; however, the majority of strong positive correlations are toward the western side of the studied region, especially during June 2013 between 94°-96°W. Figure 20 and Figure 26 are examples of western shelf locations where these correlations are strong.

4.1.4 *Hypothesis 4*

The 2011 high runoff conditions due to flooding in the upper Mississippi river basin result in statistically significant seasonal differences in carbon and nitrogen isotopic ranges in the $PO^{13}C$ and $PO^{15}N$, and in the isotopic C:N ratio.

Stable isotopes may be used to trace riverine influences along the Texas-Louisiana coast and determine the limits of coastal and marine water masses [*Dorado*, 2011]. Determination of the $d^{13}C$ and $d^{15}N$ values of POM can give us information about discrete carbon and nitrogen sources to the northern Gulf of Mexico [*Dorado*, 2011].

As water flows through an estuary, the $\delta^{13}C$ derived from $PO^{13}C$ generally increases from -30‰ to -20‰ as salinity increases, however the $\delta^{15}N$ from $PO^{15}N$ tends

to stay stable between 4‰ and 6‰ nearest the river mouth, with the Mississippi River often closer to a value of 7‰ [*Guo et al.*, 2009; *Wissel et al.*, 2005]. In the coastal environment along the Texas-Louisiana shelf, these values tend to be between 6‰ and 8‰ for ^{15}N [*Dorado*, 2011]. Low, depleted $\delta^{15}N$ values, between -1.3‰ and 1.8‰ are characteristic of true marine values [*Dorado*, 2011], and may correspond to 'blue water'.

Of the sample data herein, 47.4% of the June 2011 $PO^{15}N$ data and 42.9% of the August 2011 $PO^{15}N$ data fall in the coastal range of 6‰ to 8‰. Expanding the coastal range to include data from 4‰ (the lower range for near the river) to 9‰, 78.9% of June and 72.7% of August data fall within the coastal range. Both data sets show decreasing $PO^{15}N$ values approaching marine values, however only August 2011 reaches true marine values, likely due to the seasonal decreased river influence. All of the June and 94.5% August $PO^{13}C$ data fall within the -30‰ to -20‰ range. The August samples that exceed this range fall between -30‰ and -31‰.

Plotting the measured $\delta^{13}C$ and $\delta^{15}N$ values for the 2011 summer cruises June 2011 and August 2011, the data show a distinct negative shift in $\delta^{13}C$ values from June to August, and an increase in the ^{13}C:^{15}N ratio (Figure 37). These trends are observed both along coast (Figure 38) and within the water column. The isotope values for ^{13}C and ^{15}N are also fairly uniform throughout the water column for each cruise, with more variance in August than June (Figure 39), allowing the water column for each month to be viewed as a whole rather than splint into nominal sample depths.

The higher ^{13}C:^{15}N ratio observed in August is indicative of older organic material and decomposing material. This ratio may also be used to determine the source

of particulate matter. Using the Redfield ratio, a ratio of 6.6 indicates the phytoplankton end member and a ratio of 15 or higher is indicative of the estuarine sediment end member [*Wissel et al.*, 2005]. C:N values less than 6.6 are representative of a prominent bacterioplankton community and possibly cyanobacteria [*Wissel et al.*, 2005], and can be seen in June 2011 (Figure 37). Scatter between the phytoplankton and estuarine sediment end members may also indicate mixing between river derived sediments and the plankton community. When plotted together as one series, the June 2011 and August 2011 data also show a general trend of decreasing $\delta^{13}C$ as the ^{13}C:^{15}N ratio increases (Figure 40), however the correlation is weak, and it is not statistically significant using the Wilcoxin Rank-Sum Test (Table 8).

The ^{15}N was expected to be essentially the same seasonally (June to August 2011). To test whether these ^{15}N data are the statistically during this time period, the Wilcoxin Rank-Sum test was used as these data are not normally distributed. The null hypothesis, the ^{15}N data are statistically the same, is accepted for both the upper and lower tails after applying this test. Older, decaying material generally has a lower ^{13}C and higher C:N ratio, so the ^{13}C was expected to be higher in June 2011 than in August 2011, and C:N was expected to be lower in June 2011 than in August 2011. These parts of the hypothesis are also supported by the results of the Wilcoxin Rank-Sum test (Table 8) as the null hypothesis that they are the same is rejected.

The shift in $\delta^{13}C$ values may be caused by changing river influence as the spring freshet diminishes. The $\delta^{13}C$ values for June lie entirely within the average marine values (-18‰ to -26‰) [*Wissel et al.*, 2005], however August displays some values that

are depleted relative to these marine values. This negative shift corresponds with higher ^{13}C:^{15}N values, and may indicate an abundance of decaying material produced during the spring bloom. The August values approach the values for C_3 plants and lignite, suggesting a larger terrestrial influence [*Dorado*, 2011; *Thayer et al.*, 1983] for the source of organic matter. This may seem counterintuitive, as June receives higher riverine discharge, but the bloom associated with the higher discharge may be what drives the $\delta^{13}C$ ratio toward marine influenced values as algae produce higher $\delta^{13}C$ values [*Strauss*, 2010; *Bianchi et al.*, 2004]. The Atchafalaya branch delivers a large amount of terrestrial plant material to the northern Gulf of Mexico as it flows through marshy wetlands. Relatively lighter C_3 (average δC_3 = -27‰) material is generally deposited along the shelf nearer to shore, whereas the C_4 derived materials are generally deposited further offshore [*Strauss,* 2010; *Bianchi et al.*, 2007]. The proximity of C_3 derived materials to shore supports the terrestrial influence observed in August along the shallow shelf as those materials are broken down. Sampling locations further offshore should show more enriched values where C_4 is being respired ($\delta^{13}C$ = -20‰ to -18‰). None of sample data collected are far enough from the coastal regime to see a change in isotopic composition with latitude.

5. CONCLUSIONS

There are statistically significant differences in the quantity and composition of particulate matter (PM and POC), especially in the C:N ratio and in $\delta^{13}C$, along the Texas-Louisiana shelf during periods of flood, drought and average discharge conditions. There is no definitive direct shelf-wide relationship between particulate matter and hypoxic conditions along the shelf; however, there are some correlations between particulate matter and other factors influencing hypoxia such as sub-pycnocline chlorophyll-*a* fluorescence concentrations where no surface chlorophyll is present, suggesting production/accumulation of sub-pycnocline biomass.

Overall, Hypothesis 1: the 2012 low runoff conditions result in lower PM concentrations, lower percent and concentration of POC, and higher C:N along the shelf than during the 2013 average runoff conditions, is not supported. The PM and POC relationship was as predicted in some subareas, but this was not statistically supported throughout the shelf study area. The %POC also failed the statistical analysis for the shelf, however, C:N displayed the expected trend and was shown to be statistically valid and significant in most cases.

Hypothesis 2: POC, as well as PM are impacted by and impact hypoxic conditions in the northern Gulf of Mexico, was not statistically supported in any cases.

Hypothesis 3: Biomass, as well as resuspended sediments, are impacted by and impact hypoxic conditions in the Gulf, was not supported as a whole; however, it is valid in some areas especially towards the western end of the Texas-Louisiana shelf.

Hypothesis 4: the 2011 high runoff conditions due to flooding in the upper Mississippi river basin result in statistically significant seasonal differences in stable carbon isotopic ranges and in the stable isotopic C:N ratio in the PM, whereas stable nitrogen isotope ranges should remain the same, is valid in all cases. Future collection of stable isotopic measurements may be beneficial to research concerning nutrient cycling, or research concerning changes that occur in transition from the shelf environment to marine. There is too much variability along the coast to compare particulate matter to a regional shelf average.

Overall, the roles of PM and POC in establishing and sustaining hypoxic conditions are highly complex and further research is needed to more definitively understand the relationship between these variables. A better understanding of the actual sources of PM (i.e. is it detritus, river derived material, or resuspended sediment) would be beneficial for determining the local controls on hypoxia. It would also be beneficial to measure photosynthetically available radiation (PAR) during Acrobat tows to better assess if there is sufficient light present for biomass (measured as chlorophyll-*a*) to result from *in situ* primary production rather than older material that has settled or been resuspended.

REFERENCES

Bianchi, T. S., A.A. Mead, P. Chapman, J.H. Cowan Jr., M.J. Dagg, J.W. Day, S.F. DiMarco, R.D. Hetland, and R. Powell, 2010b, New approached to the Gulf hypoxia problem: Eos, v. 91, no. 11, p. 173-174.

Bianchi, T. S., L.A. Wysocki, M. Stewart, T.R. Fille, and B.A. McKee, 2007, Temporal variability in terrestrially-derived sources of particulate organic carbon in the lower Mississippi River and its upper tributaries: Geochimica et Cosmochimica Acta, v. 71, p. 4425-4437.

Bianchi, T. S., S.F. DiMarco, A.A. Mead, P. Chapman, J.H. Cowan Jr., R.D. Hetland, J.W. Morse, G. Rowe, 2008, Controlling hypoxia on the U.S. Louisiana shelf: beyond the nutrient-centric view: Eos, v. 89, p. 236-237.

Bianchi, T. S., S.F. DiMarco, J.H. Cowan Jr., R.D. Hetland, P. Chapman, J.W. Day, A.A. Mead, 2010a, The science of hypoxia in the Northern Gulf of Mexico: a review: Science of the Total Environment, v. 408, p.1-14.

Bianchi, T. S., T. Filley, K. Dria, and P.G. Hatcher, 2004, Temporal variability in sources of dissolved organic carbon in the lower Mississippi river: Geochimica et Cosmochimica Acta, v. 68, p. 959-967.

Cetinic, I., M.J. Perry, N.T. Briggs, E. Kallin, E.A. D'Asaro, C.M. Lee, 2012, Particulate organic carbon and inherent optics during 2008 North Atlantic Bloom Experiment: Journal of Geophysical Research, v. 117, p. C06028 1-18.

Cochran, E. M., 2013, The role of particulate matter in the development of hypoxia on the Texas-Louisiana Shelf. M.S. Thesis: Texas A&M University, p. 106

Dagg, M., R. Benner, S. Lohrenz, D. Lawrence, 2004, Transformation of dissolved and particulate materials on continental shelves influences by large rivers: plume processes: Continental Shelf Research, v. 24, p. 833-858.

Dagg, M. J., G.A. Breed, 2003, Biological effects of Mississippi River nitrogen on the northern Gulf of Mexico- a review and synthesis: Journal of Marine Systems, v. 43, p. 133-152.

Dale, V. H., C. Kling, J.L. Meyer, J. Sanders, H. Stallworth, T. Armitage, D. Wangsness, T.S. Bianchi, A. Blumberg, W. Boynton, D.J. Conley, W. Crumpton, M.B. David, D. Gilbert, R.W. Howarth, R. Lowrance, K. Mankin, J. Opaluch, H. Paerl, K. Reckhow, A.N. Sharply, T.W. Simpson, C. Synder, and D. Wright, 2010, Hypoxia in the northern Gulf of Mexico, New York, Springer, Springer Series on Environmental Management, p. 332

Diaz, R. J., 2001, Overview of hypoxia around the world: Journal of Environmental Quality, v. 30, no. 2, p. 275-281.

Diaz, R. J., and R. Rosenberg, 2008, Spreading dead zones and consequences for marine ecosystems: Science, v. 321, p. 926-929.

Diaz, R. J., and R. Rosenberg, 2011, Introduction to environmental and economic consequences of hypoxia: Water Resources Development, v. 27, no. 1, p. 71-82.

Diaz, R. J., R. Rosenberg, N.N. Rabalais, L.A. Levin, 2009, Dead zone dilemma: Marine Pollution Bulletin, v. 58, p. 1767-1768.

DiMarco, S. F. U., 2013, Mechanisms Controlling Hypoxia: Cruise Overview, Texas A&M University: College of Geosciences, http://georesearch.tamu.edu/blogs/hypoxia/cruise-overview/.

Dorado, S., 2011, Coastal and marine nitrogen sources shirt isotopic baselines in pelagic food webs of the Gulf of Mexico. M.S. Thesis: Texas A&M University- Corpus Christi, p. 59

Feng, Y., S.F. DiMarco, and G.A. Jackson, 2012, Relative role of wind forcing and riverine nutrient input on the extent of hypoxia in the northern Gulf of Mexico: Geophysical Research Letters, v. 39, p. L09601.

Forrest, D. R., R.D. Hetland, and S.F. DiMarco, 2011, Multivariable statistical regression models of the areal extent of hypoxia over the Texas-Louisiana continental shelf: Environmental Research Letters, v. 6. p. 1-10.

Gardner, W. D., 1977, Incomplete extraction of rapidly settling particles from water samplers: Limnology and Oceanography, v. 22, p. 764-768.

Gardner, W. D., C. Blakey, I.D. Walsh, M.J. Richardson, S. Pergua, J.R.V. Zaneveld, C. Roseler, M.C. Gregg, J.A. MacKinnon, H.M. Sosik, and A.J. Williams III, 2001, Optics, particles, stratification, and storms on the New England continental shelf: Journal of Geophysical Research, v. 106, p. 9473-9497.

Guo, L., D.M. White, C. Xu, and P.H. Santschi, 2009, Chemical and isotopic composition of high-molecular-weight dissolved organic matter from the Mississippi River plume: Marine Chemistry, v. 114, p. 63-71.

Hetland, R., and S. DiMarco, 2008, How does the character of oxygen control the structure of hypoxia on the Texas-Louisiana continental shelf?: Journal of Marine Systems, v. 70, p. 49-62.

Holser. R.R., M. A. Goni., and B. Hales, 2011, Design and application of a semi-automated filtration system to study the distribution of particulate organic carbon in the water column of a coastal upwelling system: Marine Chemistry, v. 123, p. 67-77.

Louisiana Universities Marine Consortium, 2014. Hypoxia In the Northern Gulf of Mexico, Louisiana Universities Marine Consortium, Chauvin, LA, http://www.gulfhypoxia.net/Overview/

Mead, A. A., C.R. Demas, B.A. Ebersole, B.A. Kleiss, C.D. Little, E.A. Meselhe, N.J. Powell, T.C. Pratt, B.M. Vosburg, 2012, A water and sediment budget for the lower Mississippi-Atchafalaya River in flood years 2008-2010: Implications for sediment discharge to the oceans and coastal restoration in Louisiana: Journal of Hydrology, v. 432-433, p. 84-97.

O'Connor, T., and D. Whitall, 2007, Linking hypoxia to shrimp catch in the northern Gulf of Mexico: Marine Pollution Bulletin, v. 54, no. 4, p. 460-463.

Quigg, A., J.B. Sylvan, A.B. Fustafson, T.R. Risher, R.L. Oliver, S. Tozzi, and J.W. Ammerman, 2011, Going West: Limitation of primary production in the northern Gulf of Mexico and the importance of the Atchafalaya River: Aquatic Geochemistry, v. 17, p. 519-544.

Rabalais, N. N., R.E. Turner, and D. Scavia, 2002, Beyond science into policy: Gulf of Mexico hypoxia and the Mississippi River: Bioscience, v. 52, p. 129-142.

Rabalais, N. N., R.J. Diaz, L.A. Levin, R.E. Turner, D. Gilbert, and J. Zhang, 2010, Dynanics and distribution of natural and human-caused hypoxia: Biogeosciences, v. 7, p. 585-619.

Rabalais, N. N., W.-J. Cai, J. Carstensen, D.J. Conley, B. Fry, X. Hu, Z. Quinones-Rovera, R. Rosenberg, C.P. Slomp, R.E. Turner, M. Voss, B. Wissel, and J. Zhang, 2014, Eutrophication- driven deoxygenation in the coastal ocean: Oceanography, v. 21, no. 1, p. 172-183.

Redfield, A. C., B.H. Ketchum, and F.A. Richard, 1963, The influence of organisms on the composition of seawater, New York, New York, Wiley, The Sea, p. 26-77.

Rossi, A., N. Massei, B. Laignel, D. Sebag, Y. Copard, 2009, The response of the Mississippi River to climate fluctuations and reservoir construction as indicated by wavelet analysis of streamflow and suspended-sediment load, 1950-1975: Journal of Hydrology, v. 377, p. 237-244.

Rowe, G. and P. Chapman, 2002, Continental Shelf hypoxia: Some nagging questions: Gulf of Mexico Science, v. 2, p. 153-160.

Schaeffer, B. A., G.A. Sinclair, J.C. Lehrter, M.C. Murrell, J.C. Kurtz, R.W. Gould, D.F. Yates, and G. Smith, 2011, An analysis of diffuse light attenuation in the northern Gulf of Mexico hypoxic zone using SeaWiFS satellite data record: Remote Sensing of Environment, v. 115, p. 3748-3757.

Strauss, J., 2010, Stable isotope characterization and proxy records of hypoxia-susceptible waters on the Texas-Louisiana shelf. PhD Dissertation: Texas A&M University, p. 139

Thayer, G. W., J.J. Govoni, and D.W. Connally, 1983, Stable carbon isotope ratios of the planktonic food web in the northern Gulf of Mexico: Bulletin of Marine Science, v. 33, p. 247-256.

Turner, R. E., N.N. Rabalais, R.B Alexander, G. McIsaac, and R.W. Howarth, 2007, Characterization of nutrient, organic carbon, and sediment loads and concentrations from the Mississippi River into the northern Gulf of Mexico: Estuaries and Coasts, v. 30, no. 5, p. 773-790.

United States Geological Survey, 2014, USGS 07374000 Mississippi at Baton Rouge, LA, http://nwis.waterdata.usgs.gov.

Wissel, B., A. Gace, and B. Fry, 2005, Tracing river influences on phytoplankton dynamics in two Louisiana estuaries: Ecology, v. 86, no. 10, p. 2751-2762.

APPENDIX A

FIGURES

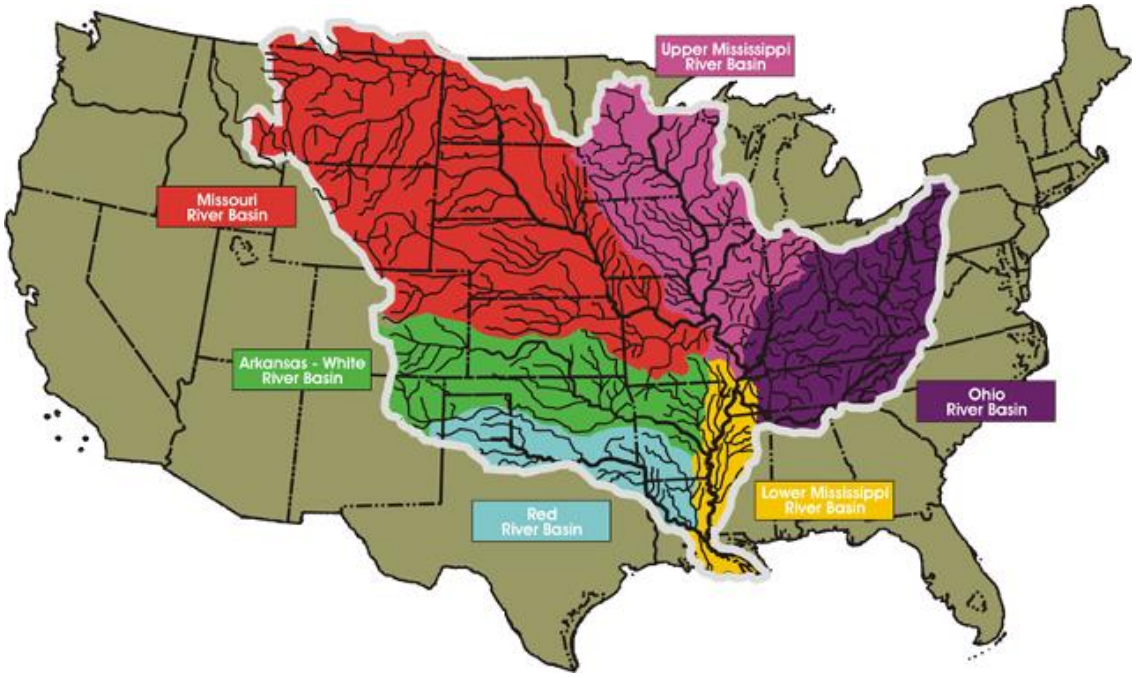

Figure 1: Extent of the Mississippi River Basin. The Mississippi river basin covers 40% of North America, and is divided into six sub-basins as displayed above. Figure from the Louisiana Universities Marine Consortium [2014].

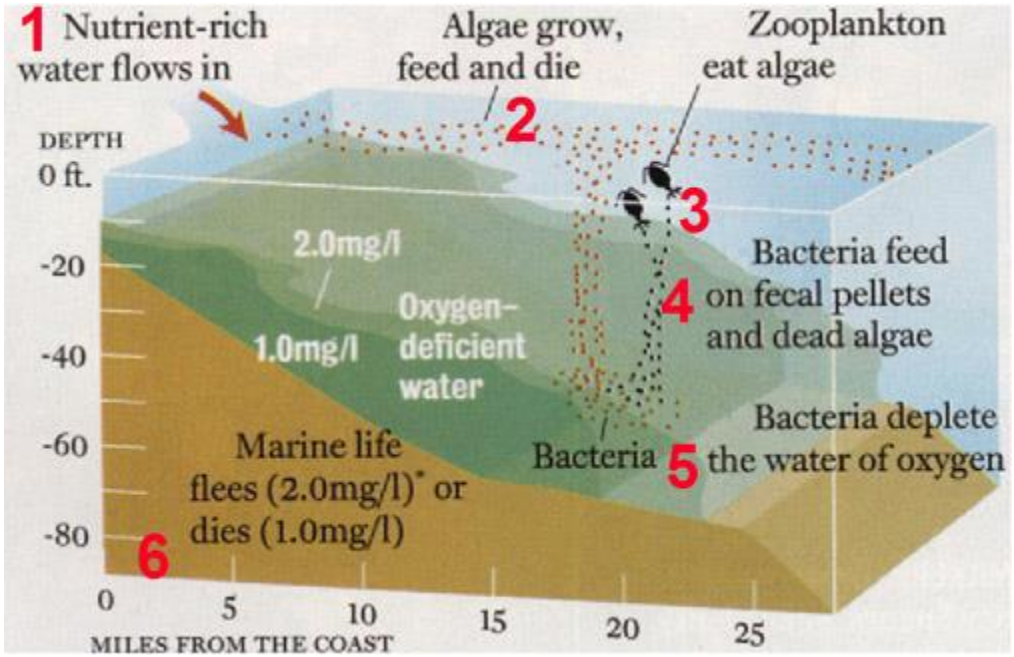

Figure 2: Nutrient-based Hypoxia Formation. 1) Nutrient-rich fresh water flows in, strongly stratifying the water column, 2) Algae grow, feed, and die, 3) Zooplankton eat the algae, 4) Bacteria feed on fecal pellets and dead algae, 5) Bacteria deplete the underlying sub-pycnocline water of oxygen, while strong stratification prevents ventilation of the lower water column 6) Marine life flees or dies. Figure from the Louisiana Universities Marine Consortium [2014].

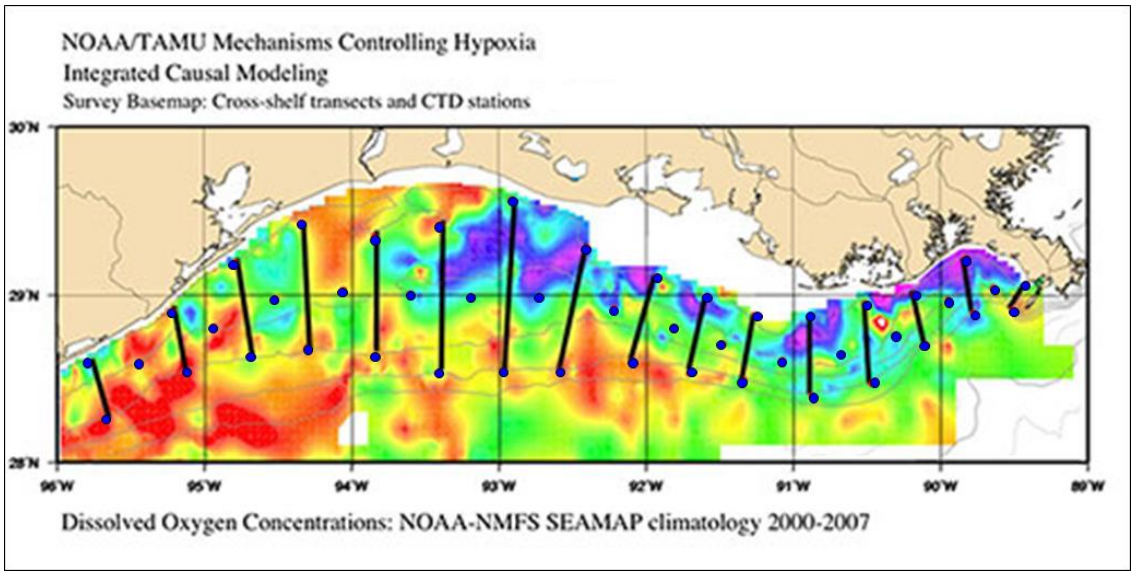

Figure 3: Hypoxia Climatology 2000-2007 for the Northern Gulf of Mexico. Dissolved oxygen concentration in the Northern Gulf of Mexico averaged from 2000-2007 (red: high oxygen; blue and violet: hypoxic). CTD casts were planned at blue dot stations. Thick black lines represent cross-shelf transects with an undulating towed vehicles. Bottom oxygen concentrations are based on NOAA-NMFS SEAMAP averaged summer survey data 2000-2007 [*DiMarco*, unpublished].

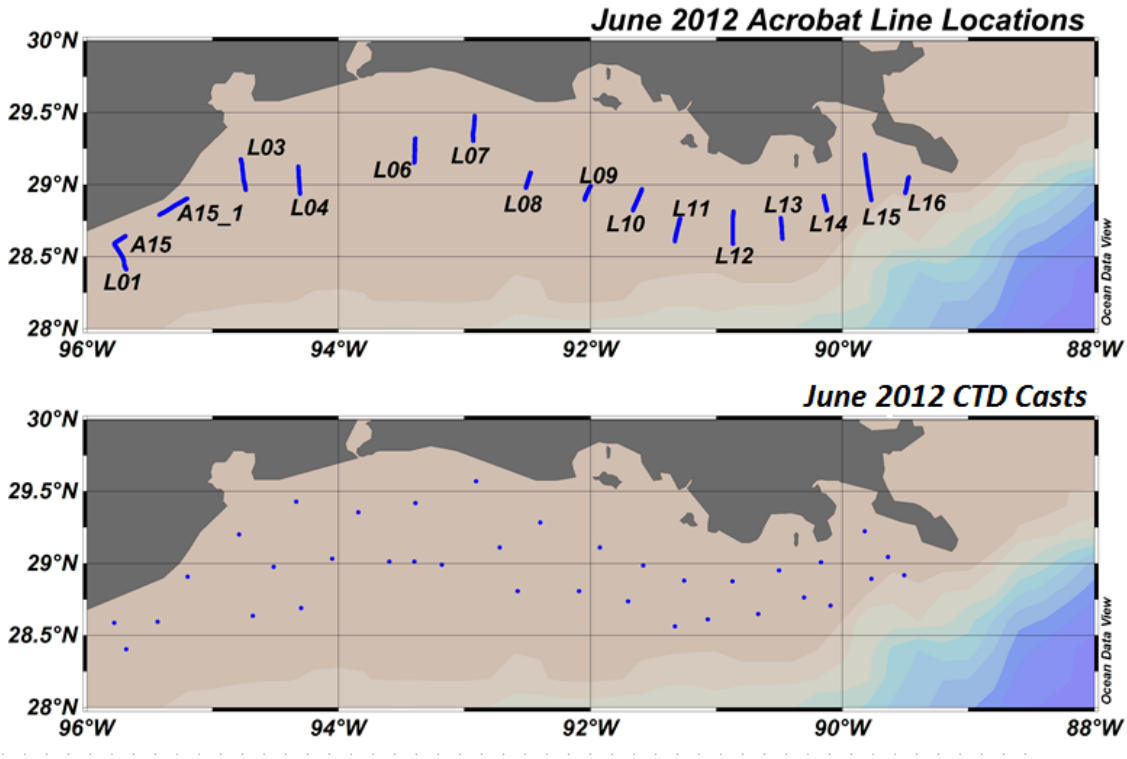

Figure 4: June 2012 Acrobat and CTD Locations. Acrobat lines (top map) and all CTD casts (bottom map) during the June 2012 cruise.

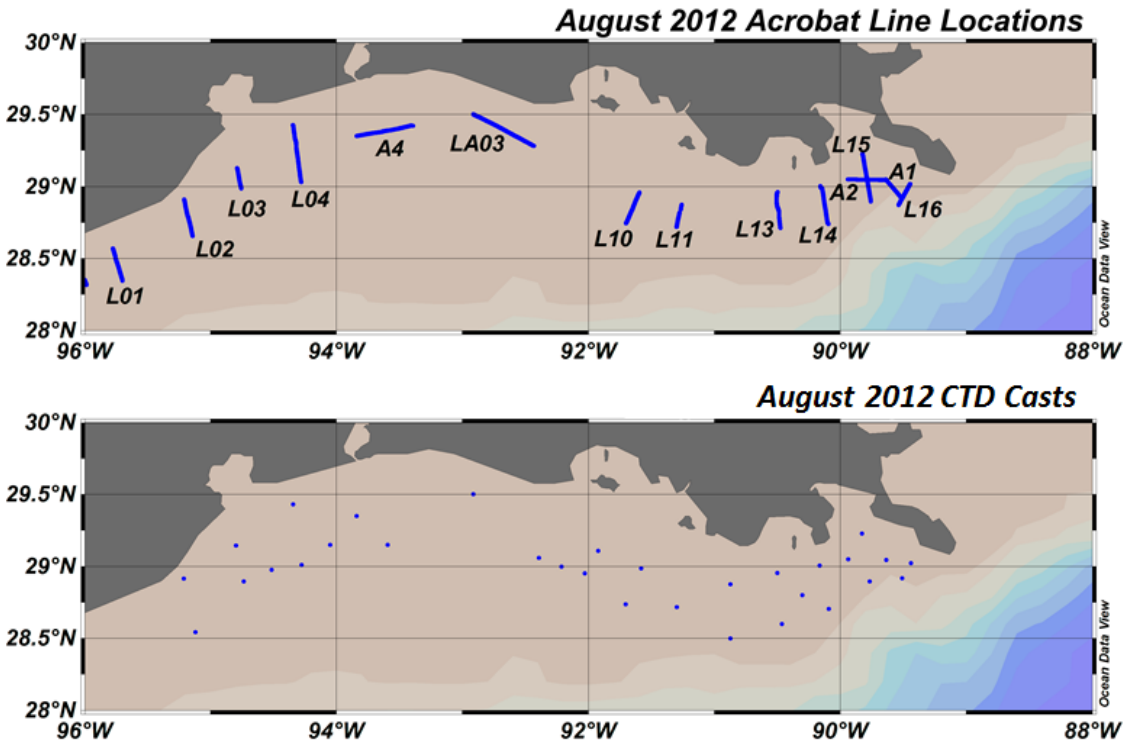

Figure 5: August 2012 Acrobat and CTD Locations. Acrobat lines (top map) and all CTD casts (bottom map) during the August 2012 cruise.

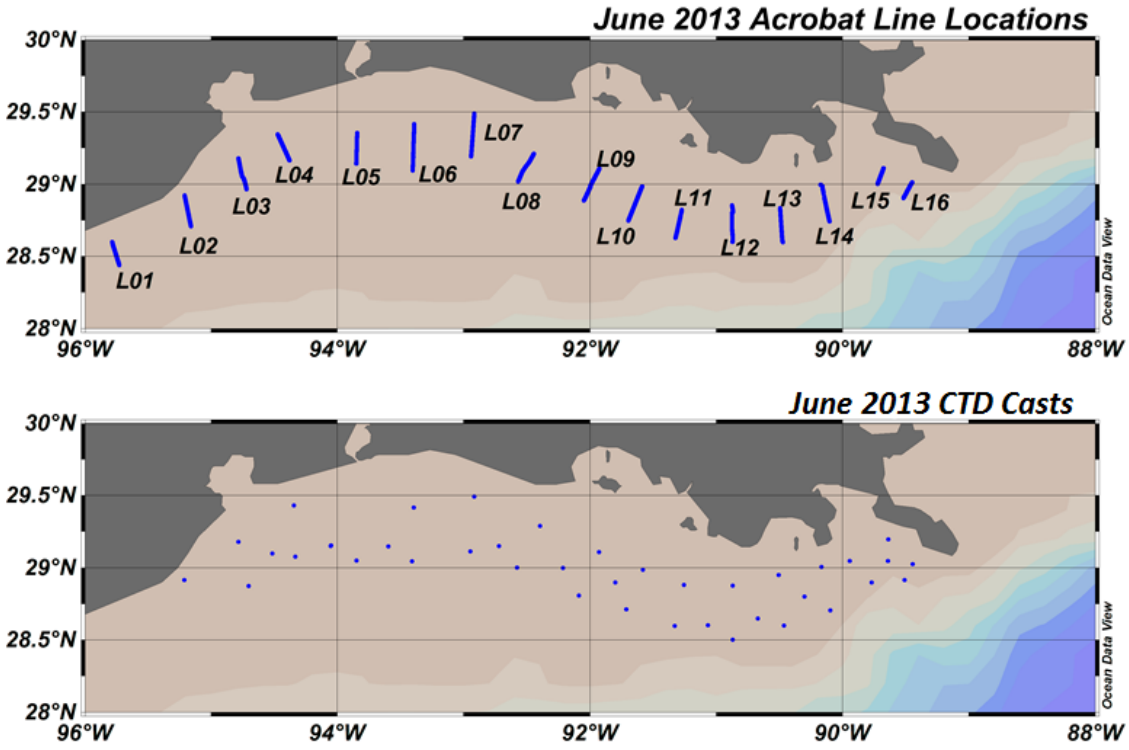

Figure 6: June 2013 Acrobat and CTD Locations. Acrobat lines (top map) and all CTD casts (bottom map) during the June 2013 cruise.

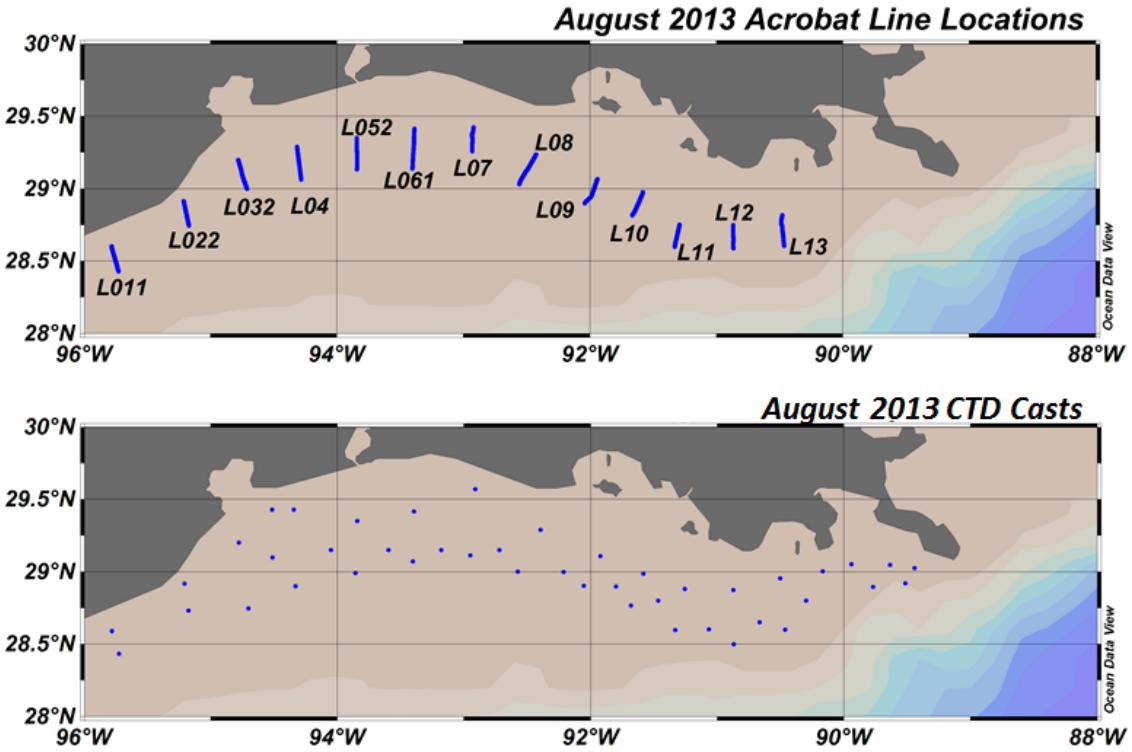

Figure 7: August 2013 Acrobat and CTD Locations. Acrobat lines (top map) and all CTD casts (bottom map) during the August 2013 cruise. Note that the Acrobat was not towed beyond 90°W during this cruise.

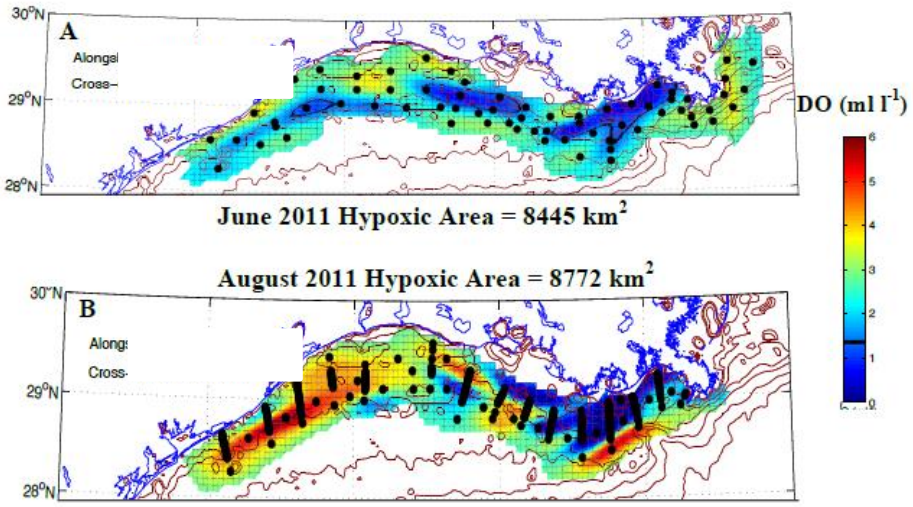

Figure 8: Maps Displaying Bottom Water Hypoxia. A) June 2011 and B) August 2011. The calculated total hypoxic area is very similar for both months; however, the bottom waters along the shelf are much closer to the hypoxic threshold during June. August displays much larger areas of well oxygenated water along the shelf [*S.F. DiMarco*, personal communication].

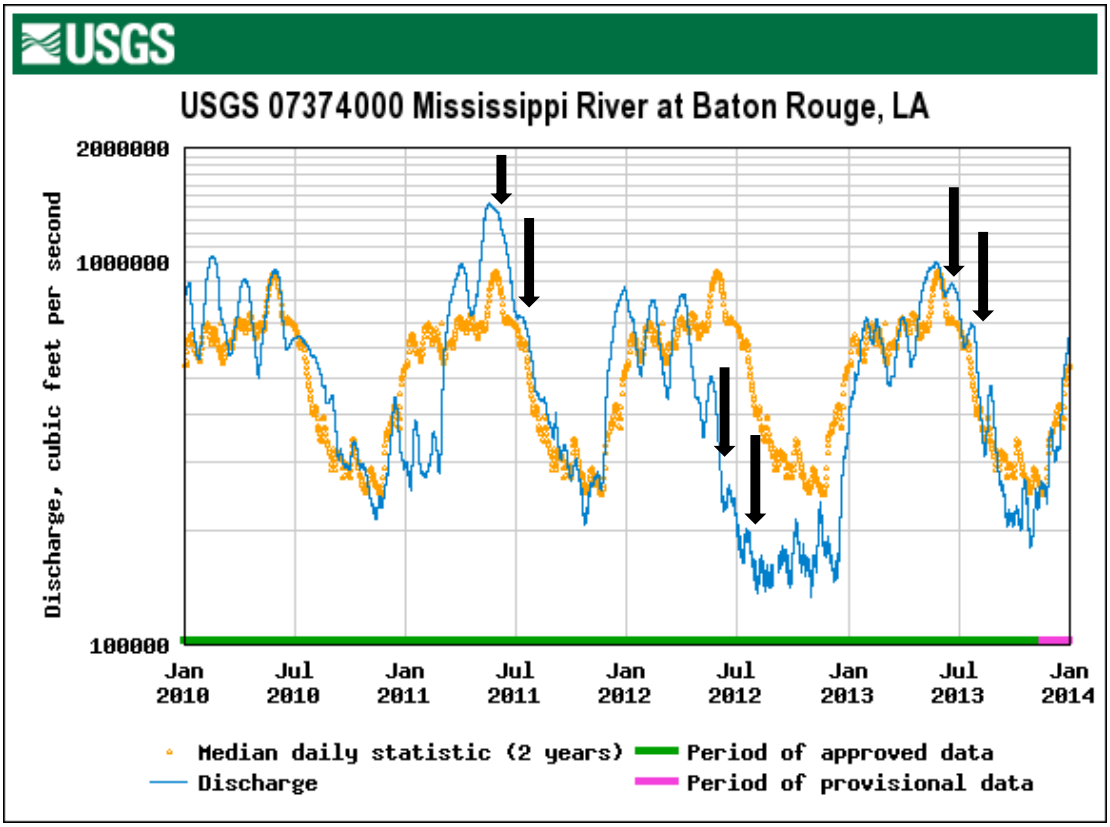

Figure 9: Mississippi River Discharge at Baton Rouge. The daily mean discharge (blue line) from January 1, 2010 through December 31, 2013 versus the mean daily statistic (yellow dots) averaged over a 7 year period for the Mississippi River measured at USGS Station 07374000 at Baton Rouge, LA [*USGS*, 2014]. Note the discharge scale is logarithmic. The black arrows point to the data for the approximate dates of each cruise. The arrows left to right represent June 2011, August 2011, June 2012, August 2012, June 2013, and August 2012.

The spring 2011 discharge is well above the 7-year average, and remains approximately 20% above the average through summer 2011. The discharge from April-December is well below the long-term average discharge resulting from drought conditions in the Mississippi River watershed. The discharge is approximately 20% greater than the long-term average in May-June 2013, and about the long-term average from July-September 2013. Data from USGS [2014, http://nwis.waterdata.usgs.gov].

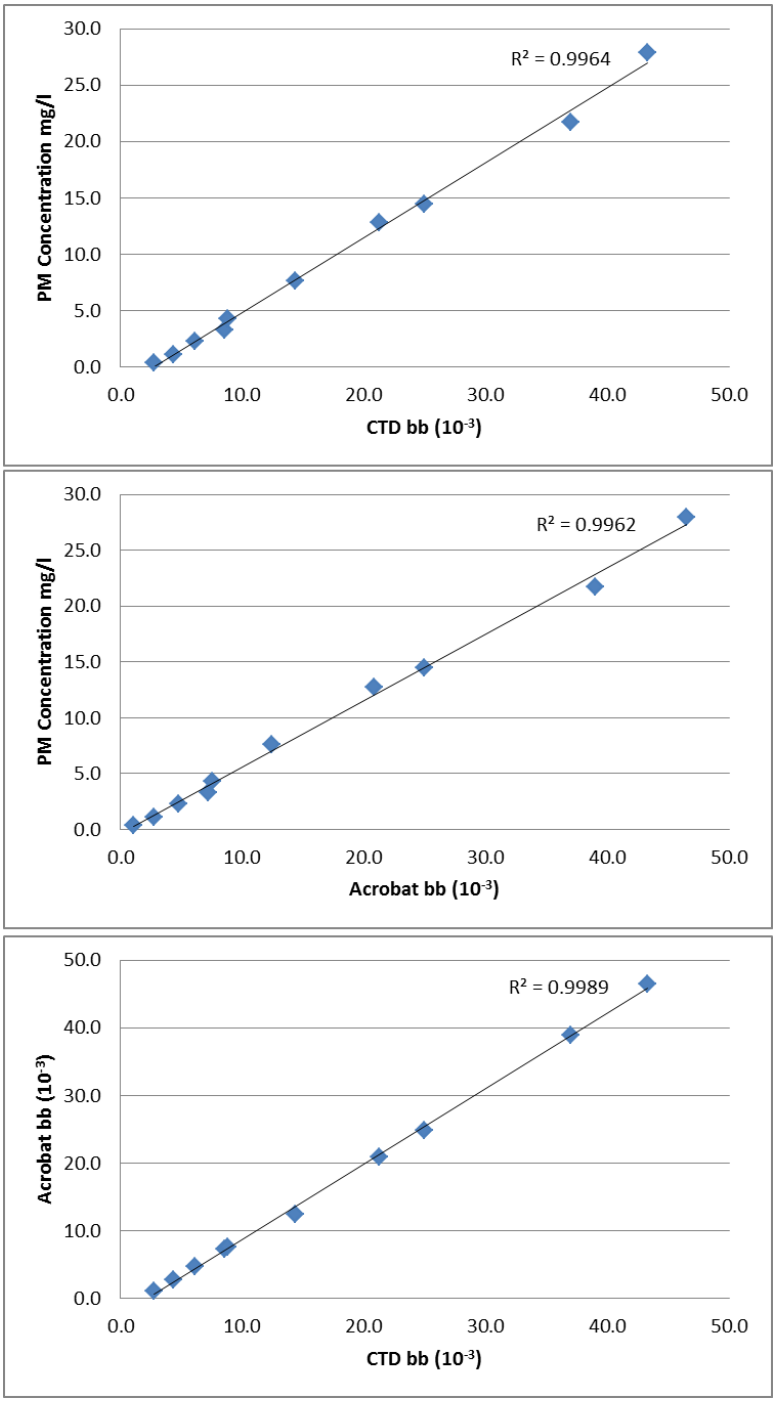

Figure 10: Laboratory calibration of PM. PM (sediment diameter < 8µm) vs. backscatter for the CTD (top) and Acrobat (middle) FLNTU instruments, and backscatter of the CTD FLNTU vs. the Acrobat FLNTU (bottom).

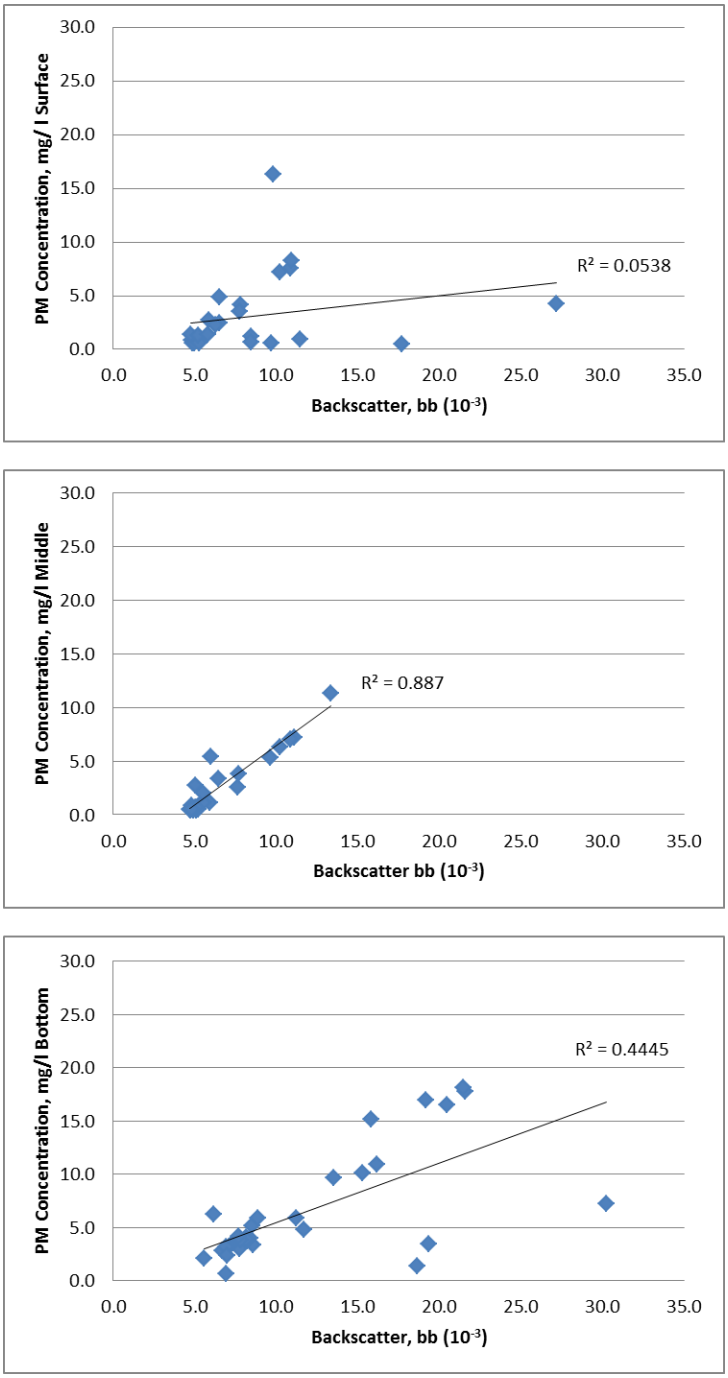

Figure 11: June 2012 Field PM Calibration. PM vs. backscatter for the CTD FLNTU instruments for June 2012. From top to bottom, these calibrations are for the surface, middle, and bottom sample depths.

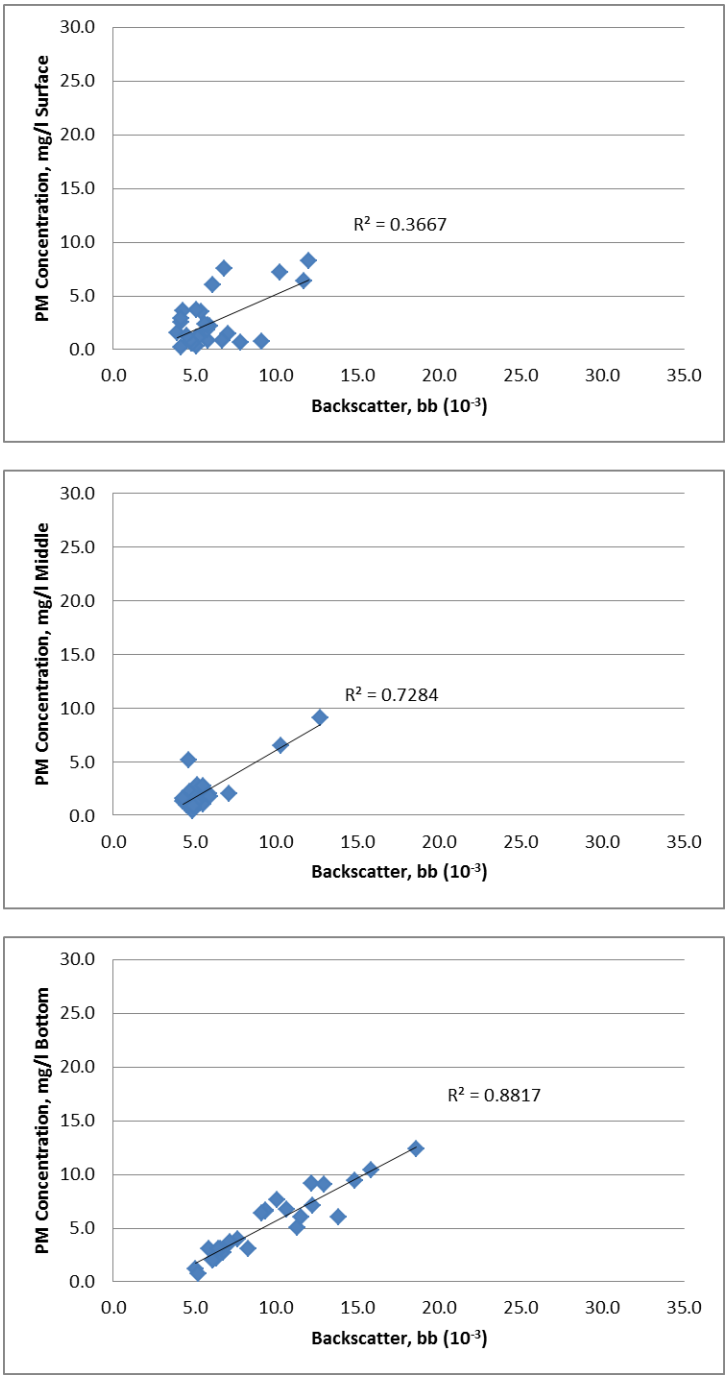

Figure 12: August 2012 Field PM Calibration. PM vs. backscatter for the CTD FLNTU instruments for August 2012. From top to bottom, these calibrations are for the surface, middle, and bottom sample depths.

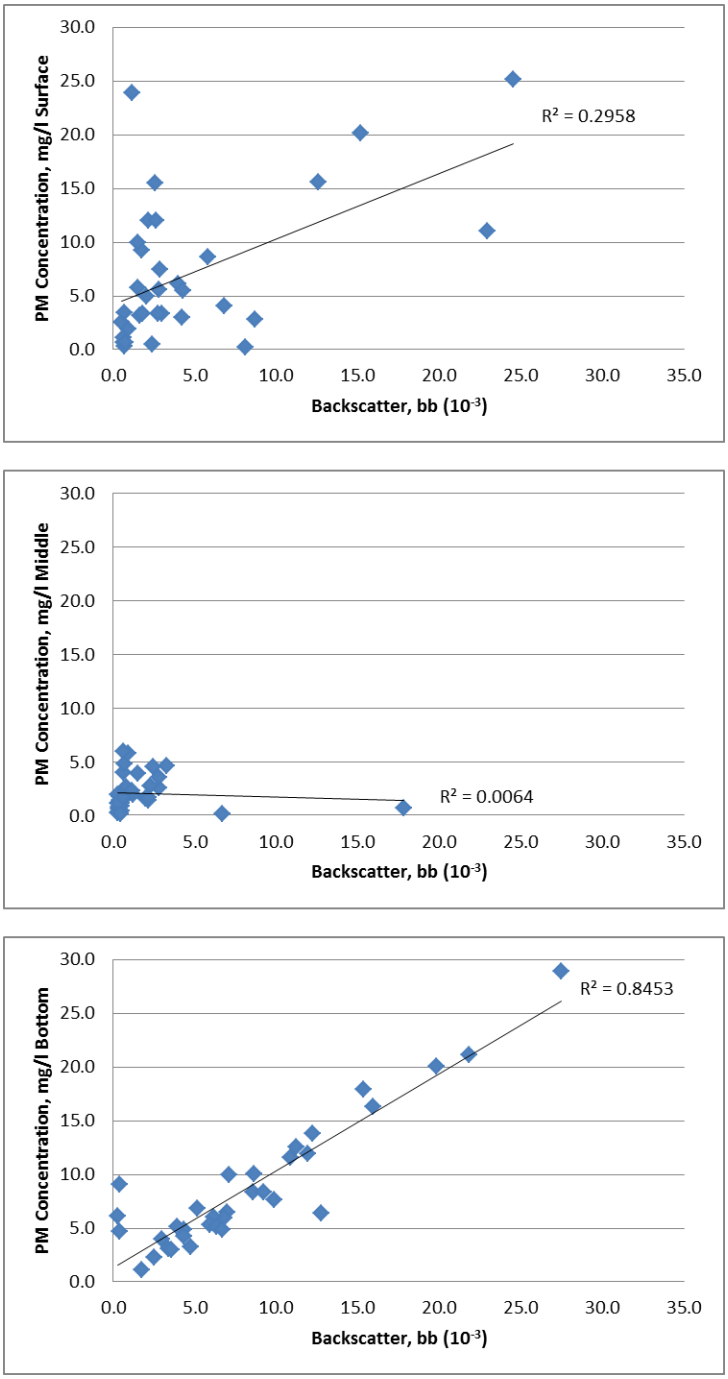

Figure 13: June 2013 Field PM Calibration. PM vs. backscatter for the CTD FLNTU instruments for June 2013. From top to bottom, these calibrations are for the surface, middle, and bottom sample depths.

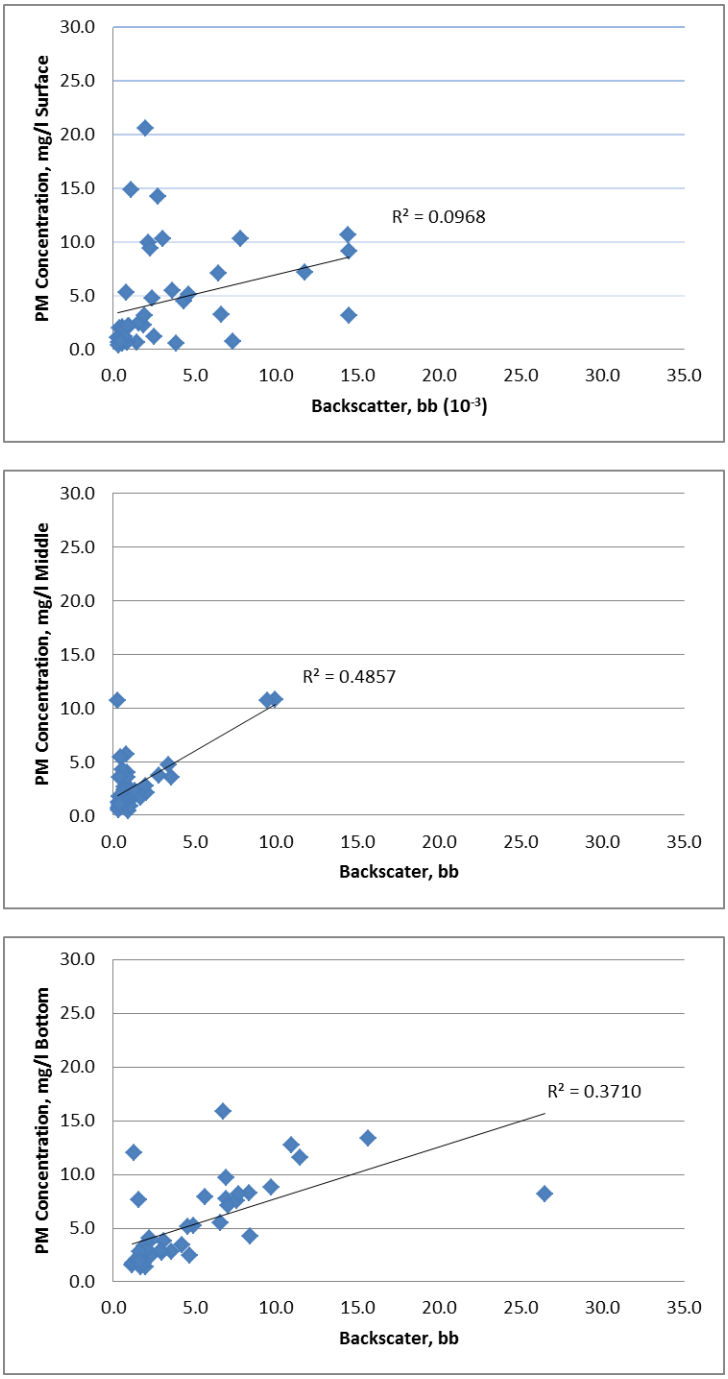

Figure 14: August 2013 Field PM Calibration. PM vs. backscatter for the CTD FLNTU instruments for August 2013. From top to bottom, these calibrations are for the surface, middle, and bottom sample depths.

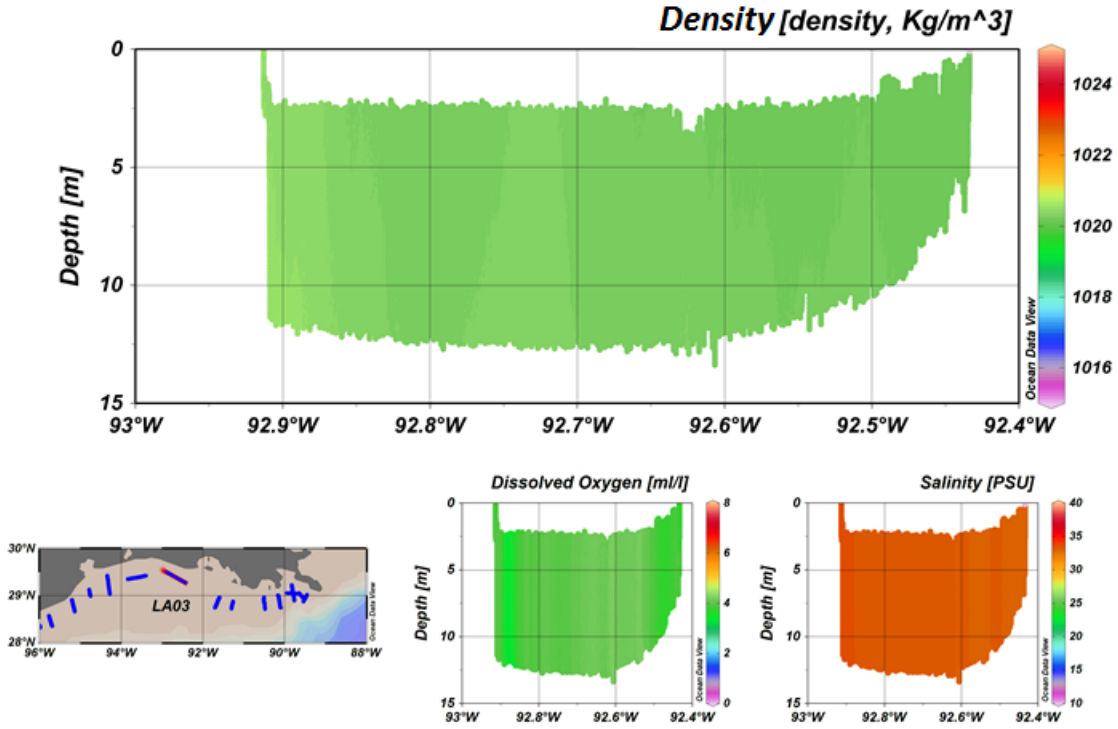

Figure 15: Well Mixed Water Column. Example sections of a well-mixed water column, as indicated by density, dissolved oxygen, and salinity. These sections are from line LA03 during August 2012.

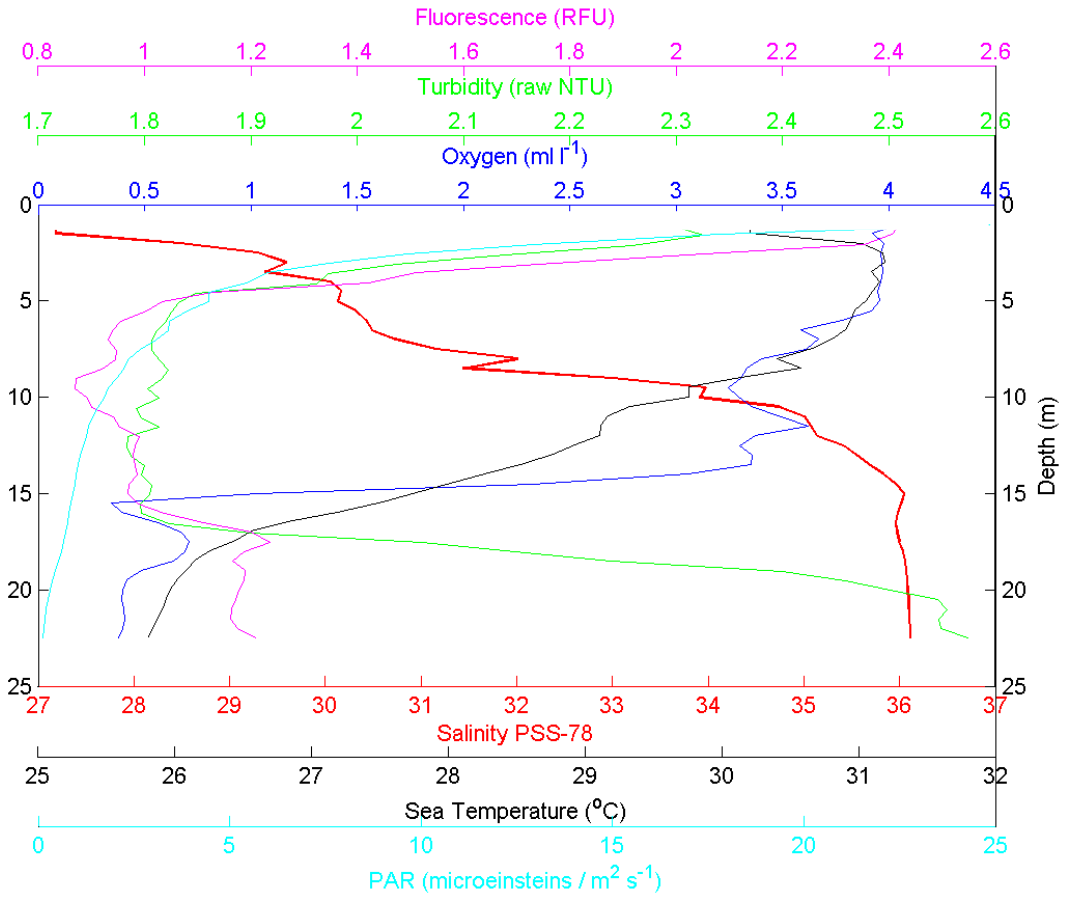

Figure 16: 'Green' Zone Profile. This CTD profile from August 2012 (MS06-A02) is an example of the 'green' zone. Note the high chlorophyll fluorescence (magenta) at the surface decreasing with depth. The dissolved oxygen concentration (blue line) also decreases with depth below the pycnocline, indicated by the salinity (red line). The increase in turbidity (green line) near bottom is likely due to resuspension of sediments.

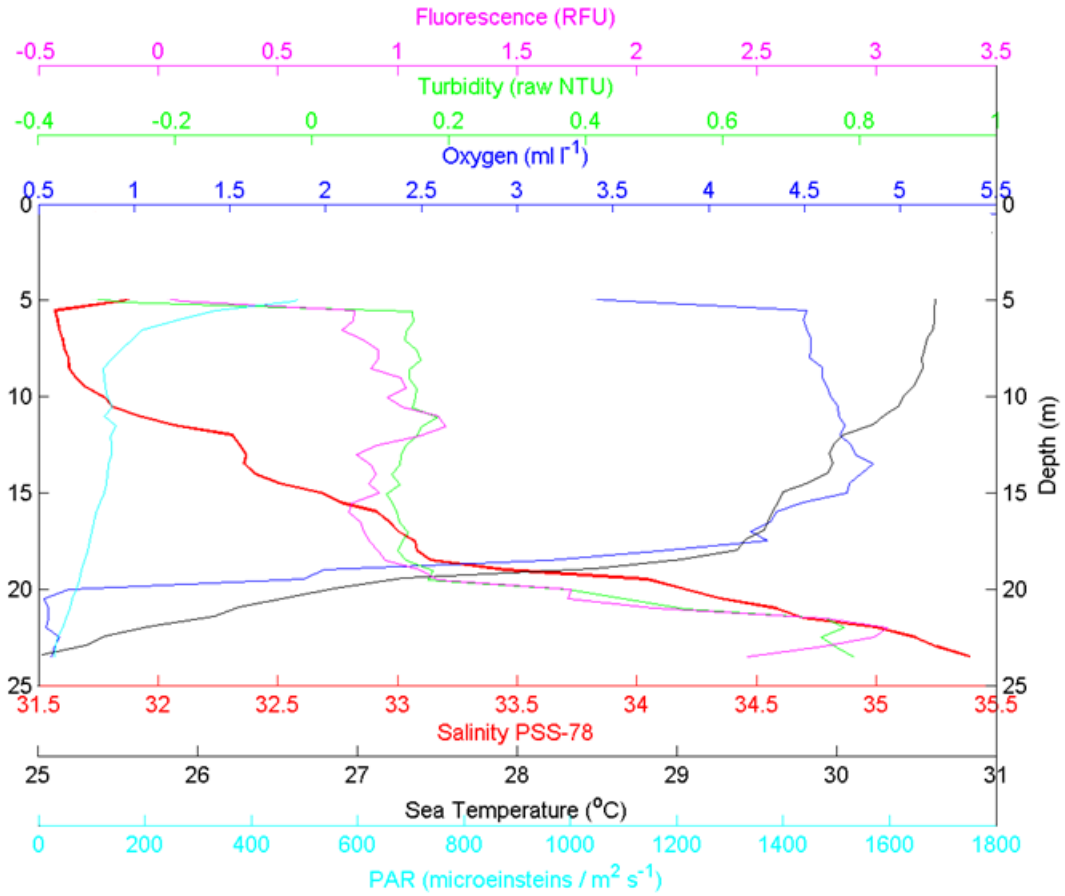

Figure 17: 'Blue' Zone Profile. This CTD cast from August 2013 (MS08-L082) is an example of the 'blue' zone. Chlorophyll fluorescence (magenta line) increases below the pycnocline, indicated by salinity (red line). At this depth, dissolved oxygen concentration (blue line) also decreases below the hypoxic threshold, due to net respiration that is higher than net production.

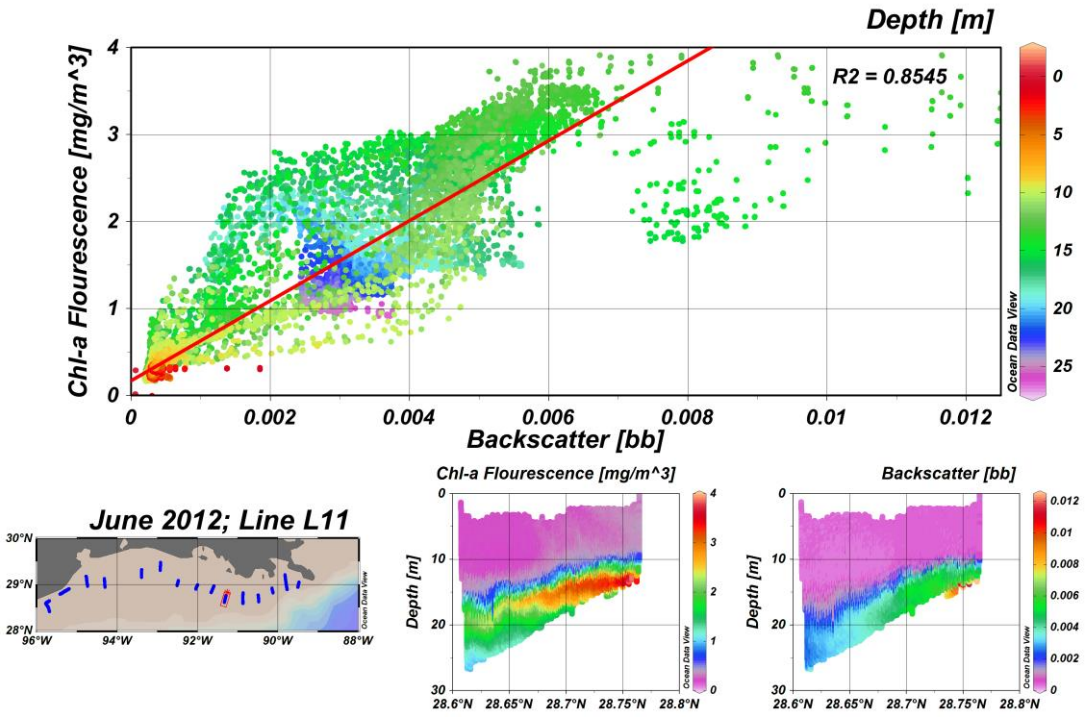

Figure 18: June 2012 Line L11 Chl-*a* Fluorescence and Backscatter. Line L11 (highlighted in red in the map), south of East Cote Blanche and Atchafalaya Bays, during June of 2012. This line displays high sub-pycnocline chlorophyll-*a* flourescence corresponding with high bottom turbidity measured by proxy as backscatter.

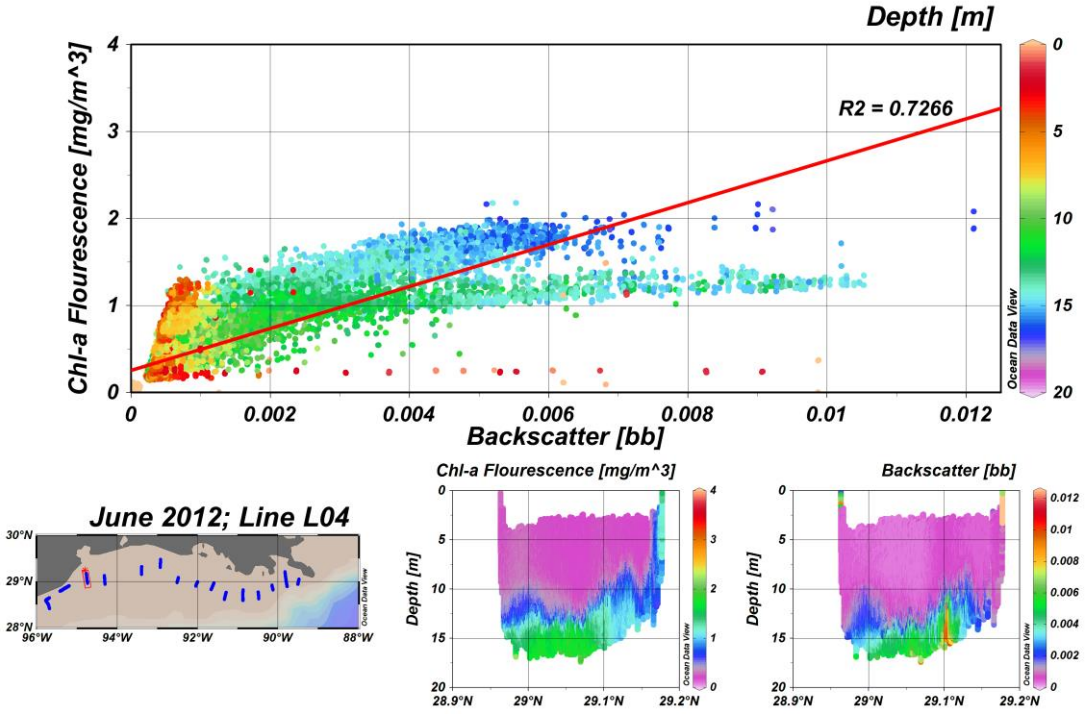

Figure 19: June 2012 Line L3 Chl-*a* Fluorescence and Backscatter. Line L3 (highlighted in red in the map), south of Galveston, during June of 2012. This line displays high sub-pycnocline chlorophyll-*a* flourescence corresponding with high bottom turbidity measured by proxy as backscatter.

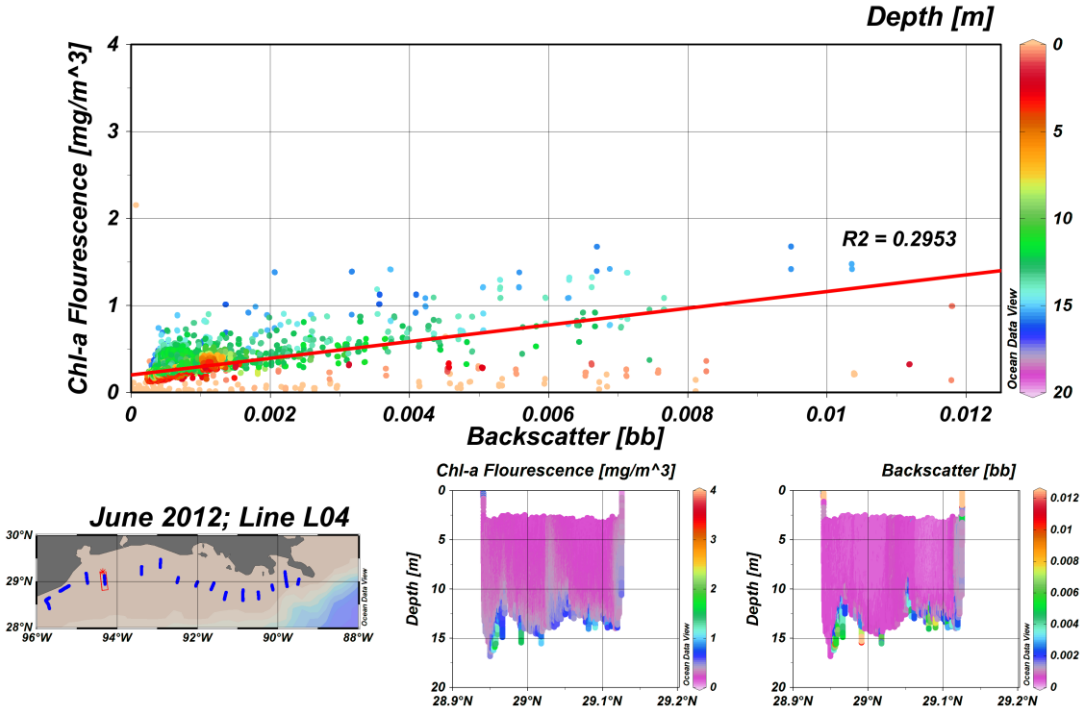

Figure 20: June 2012 Line L04 Chl-*a* Fluorescence and Backscatter. Line L04 (highlighted in red in the map), south of Galveston, during June of 2012. This line displays resuspension of sediments increasing sub-pycnocline turbidity, in addition to a small increase in chlorophyll fluorescence.

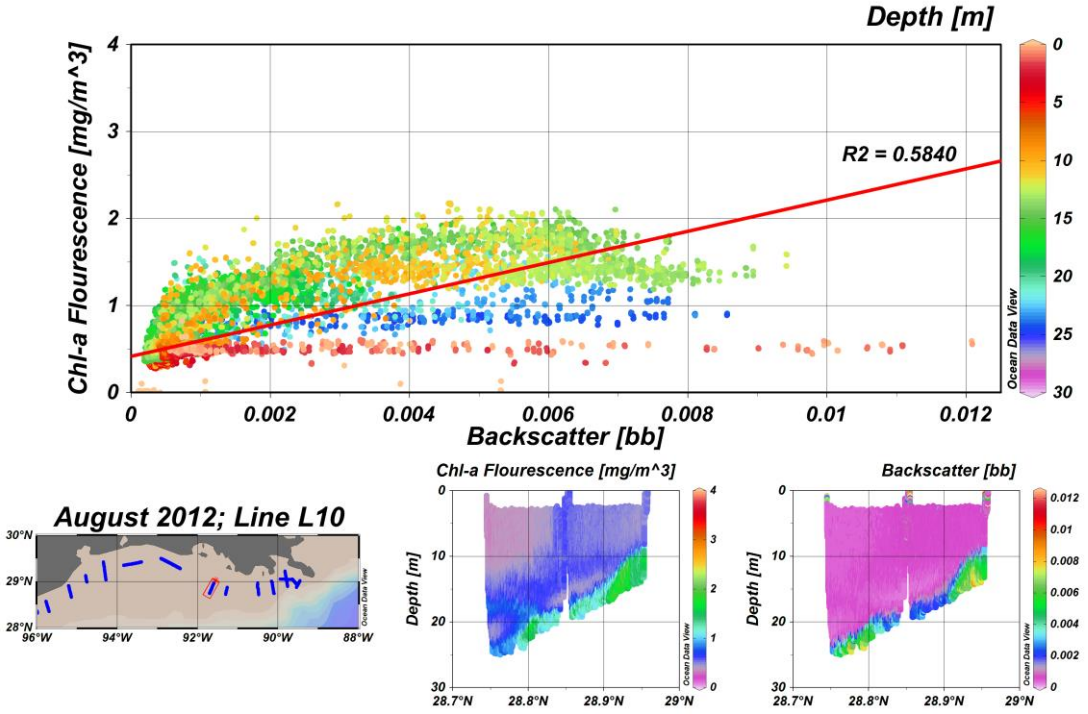

Figure 21: August 2012 Line L10 Chl-*a* Fluorescence and Backscatter. Line L10 (highlighted in red in the map), south of East Cote Blanche Bay, during August of 2012. This line displays high sub-pycnocline chlorophyll-*a* flourescence corresponding with high bottom turbidity measured by proxy as backscatter.

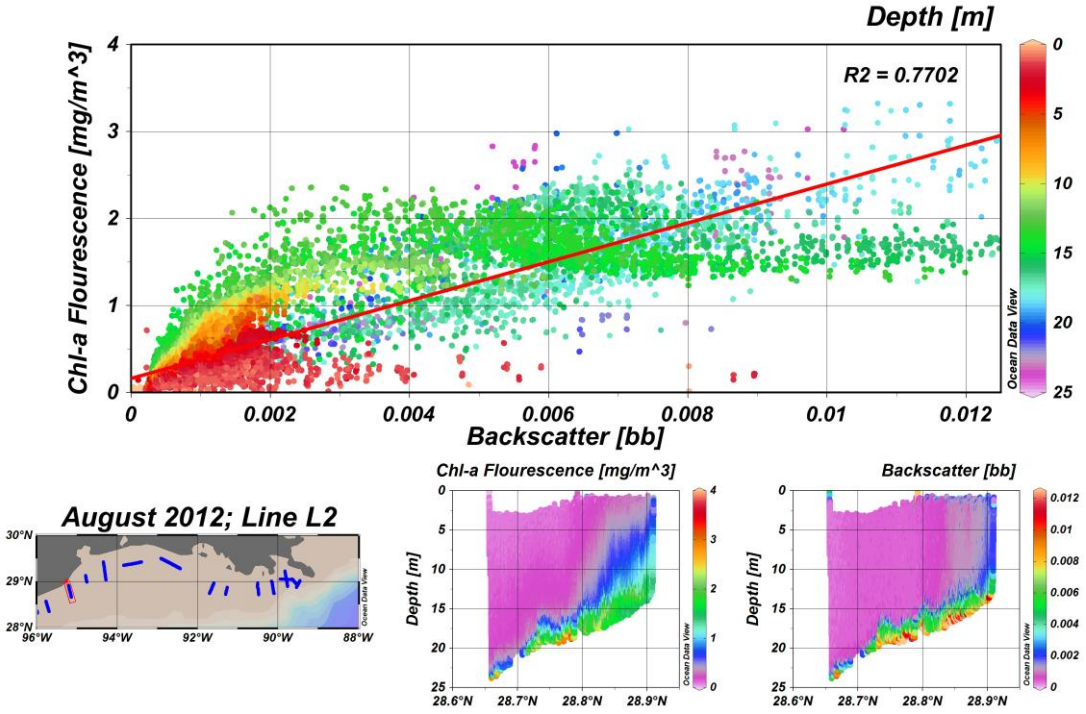

Figure 22: August 2012 Line L2 Chl-*a* Fluorescence and Backscatter. Line L2 (highlighted in red in the map), south of Galveston, during August of 2012. This line displays high sub-pycnocline chlorophyll-*a* flourescence corresponding with high bottom turbidity measured by proxy as backscatter.

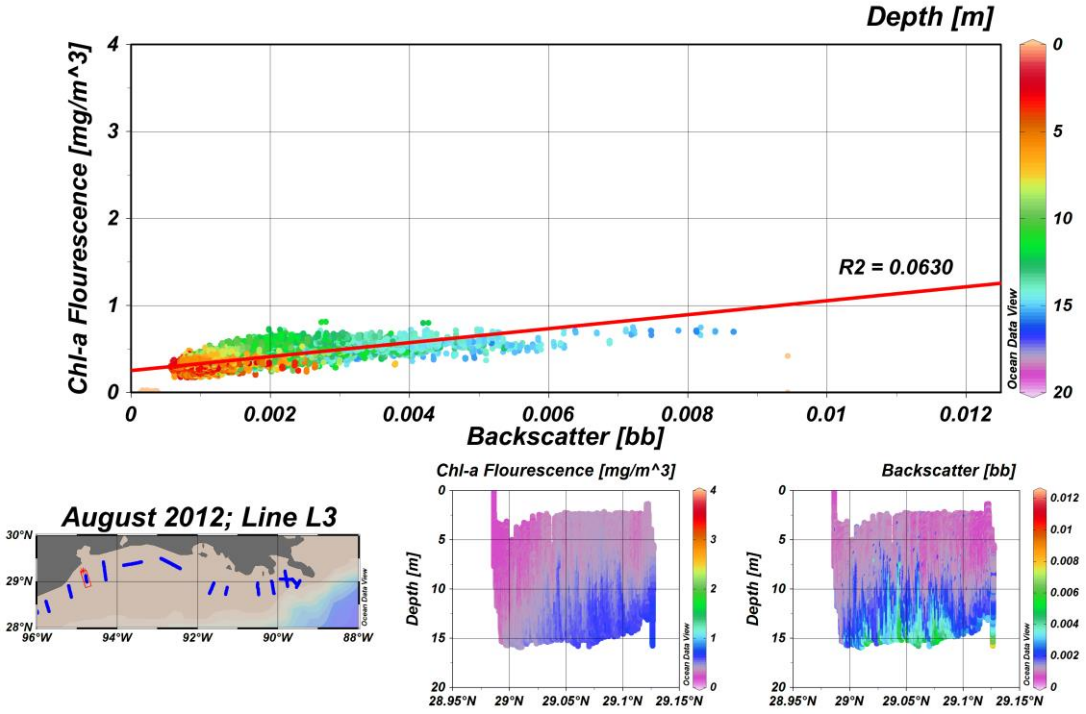

Figure 23: August 2012 Line L3 Chl-*a* Fluorescence and Backscatter.L3 (highlighted in red in the map), south of Galveston, during August of 2012. Alhough this line displayed high bottom chlorophyll flourescence during June 2012, it dispayed high sub-pycnocline turbidity likely due primairly to resuspension of sediments and minimal chlorophyll flourescence during Augus 2012.

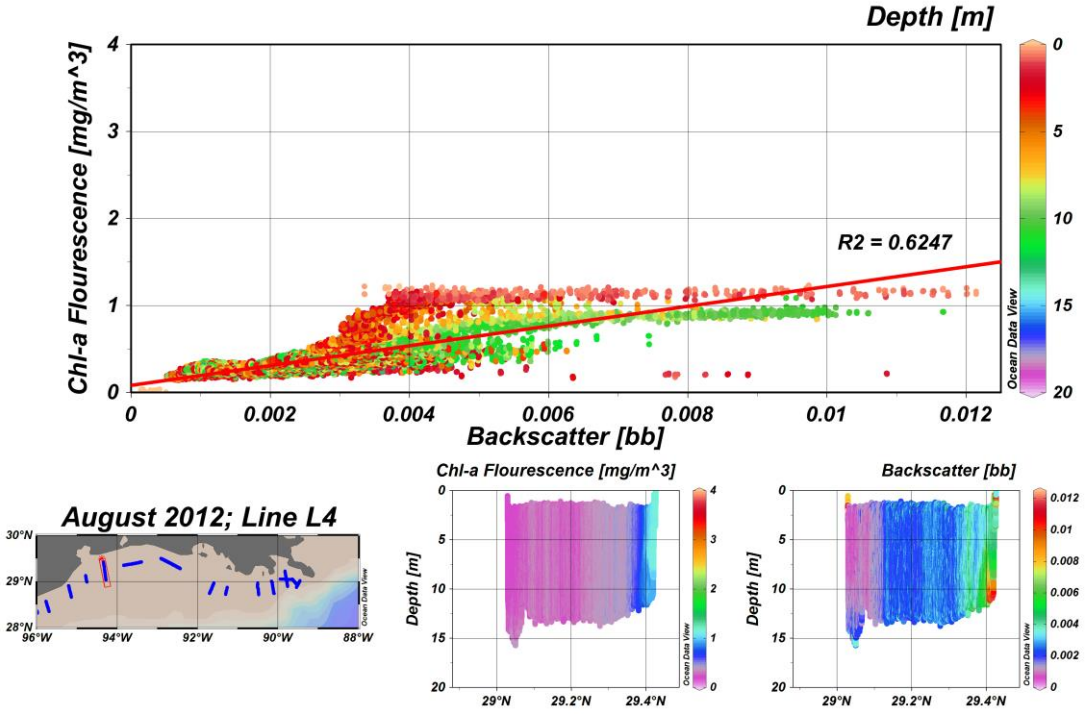

Figure 24: August 2012 Line L04 Chl-*a* Fluorescence and Backscatter. L04 (highlighted in red in the map), south of Galveston, during August of 2012. This line displays increased turbidity throughout the water column, with only a small increase in chlorophyll-*a* fluorescence on the landward end of the line.

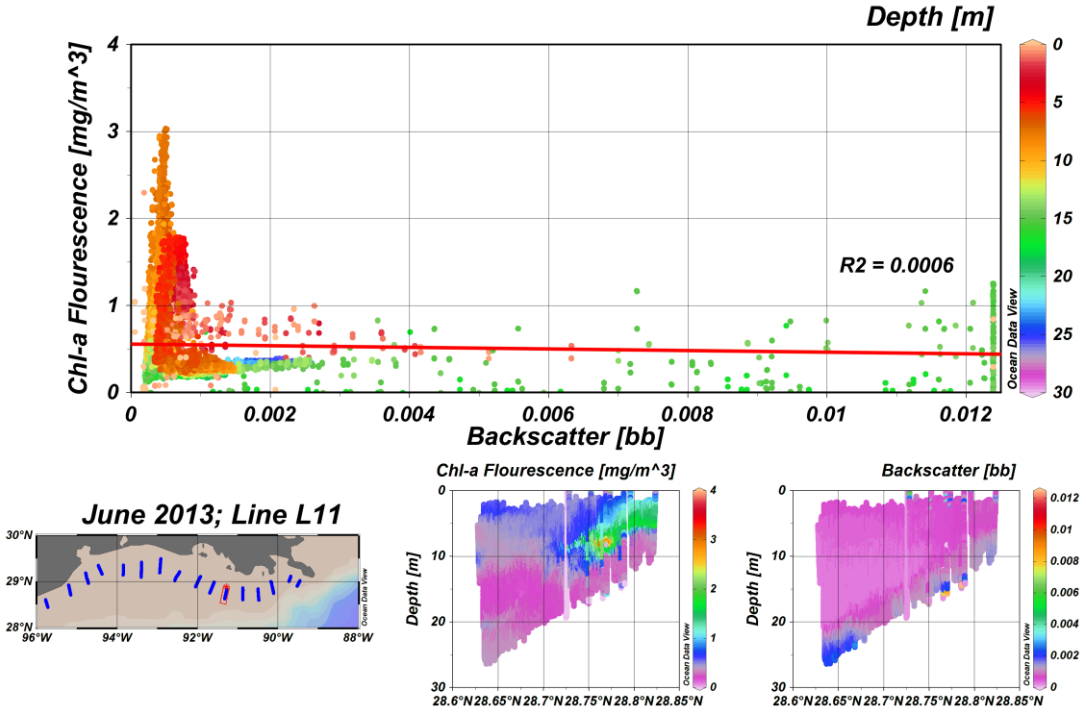

Figure 25: June 2013 Line L11 Chl-*a* Fluorescence and Backscatter. Line L11 (highlighted in red in the map), south of East Cote Blanche Bay and Atchafalaya Bay, during June of 2013. This line displays a mid-water maximum in chlorophyll-*a* flourescence on the near-shore region of the line, and high sub-pycnocline turbidity from resuspension at the off-shore region of the line.

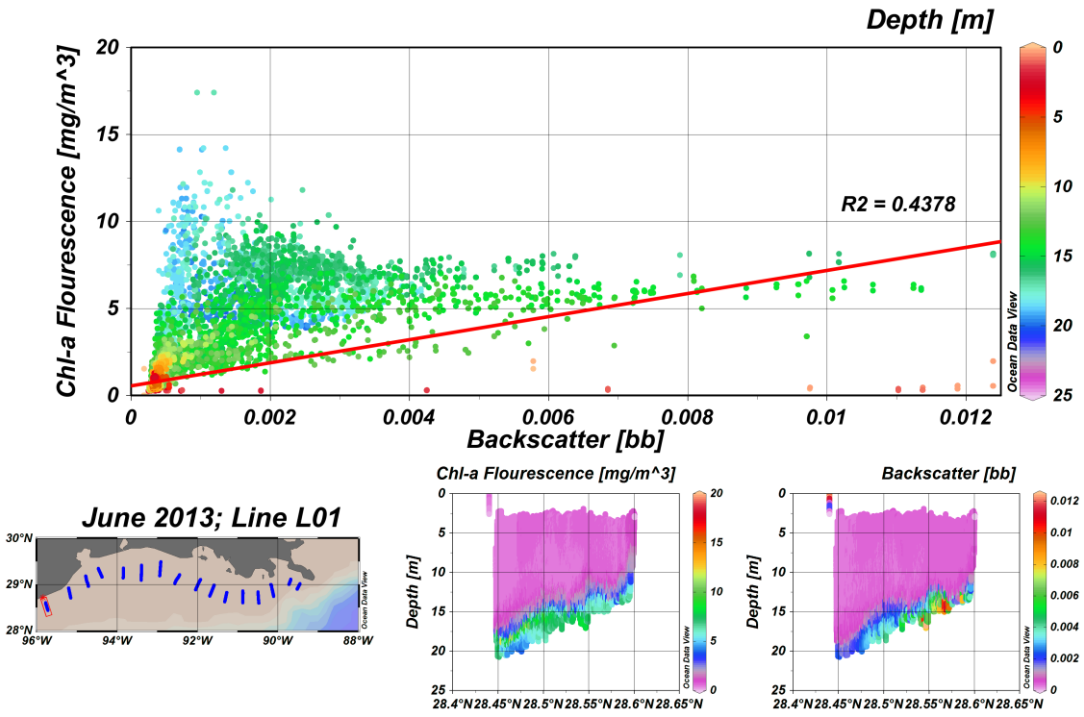

Figure 26: June 2013 Line L01 Chl-*a* Fluorescence and Backscatter. Line L01 (highlighted in red in the map), south of Galveston, during August of 2012. This line displays highly variable correspondence of sub-pycnocline chlorophyll-*a* flourescence with high bottom turbidity measured by proxy as backscatter.

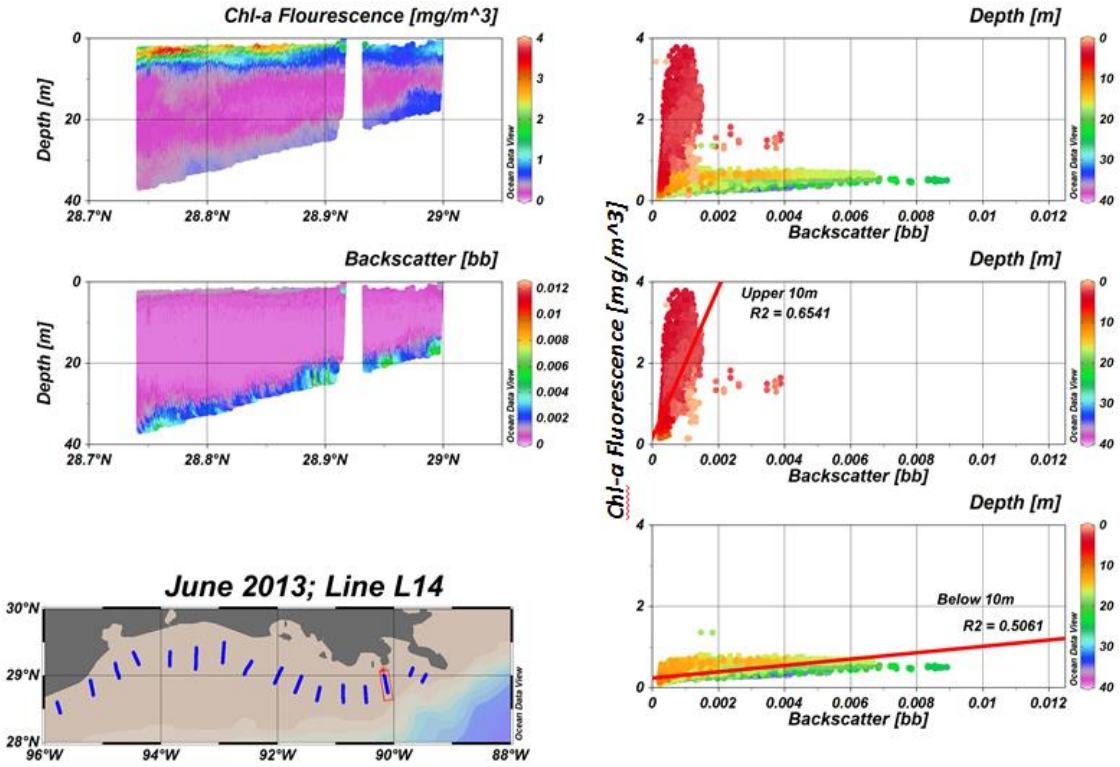

Figure 27: June 2013 Line L14 Chl-*a* Fluorescence and Backscatter. Line L14 (highlighted in red in the map), southwest of the Mississippi Delta, during June of 2013. The scatter plot (top right) was split at the 10m depth interval to separate the surface (middle right) and bottom (bottom right) trends. This line displays high near bottom turbidity measured by proxy as backscatter with negligible increase in chlorophyll-*a* flourescence, where as the high surface water chlorophyll-*a* flourescence corresponds with a slight increase in bb. Light atteneatuion by high surface chlorophyll flourescence particles and the greater bottom depth may influence the lack of flourescence production in sub-pycnocline waters. The gap in the section is due to retrieving the Acrobat to check its sensors after it hit bottom on one of its undulations.

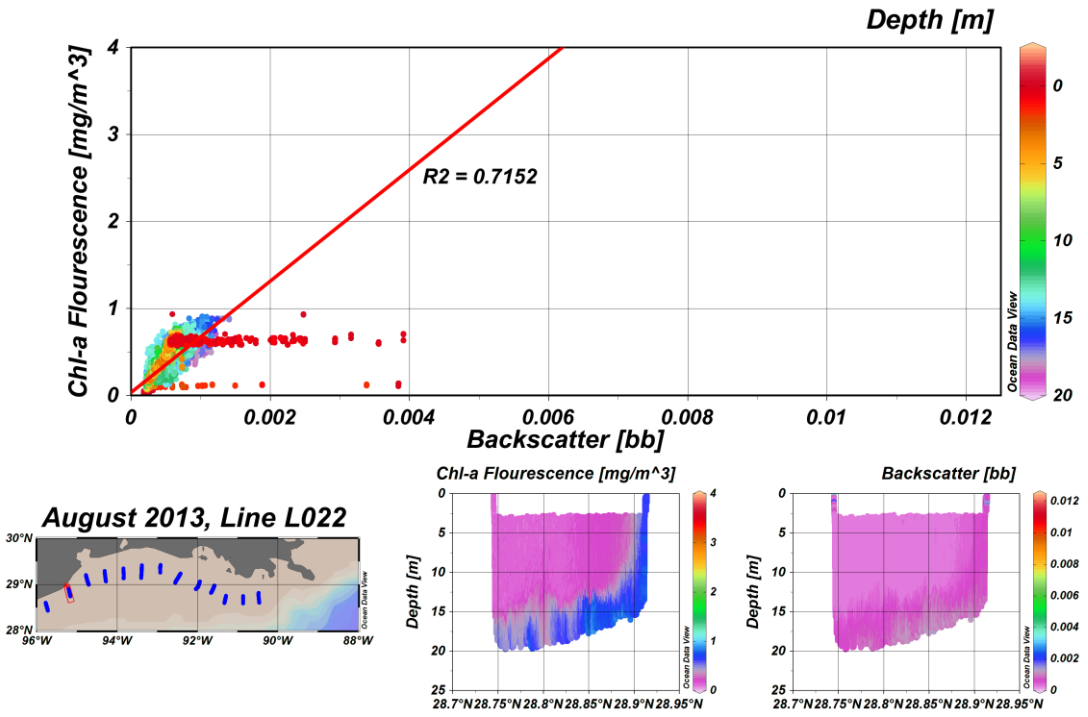

Figure 28: August 2013 Line L022 Chl-*a* Fluorescence and Backscatter. Line L022 (highlighted in red in the map), south of Galveston, during Agust of 2013. This line displays high sub-pycnocline chlorophyll-*a* flourescence corresponding with high bottom turbidity measured by proxy as backscatter.

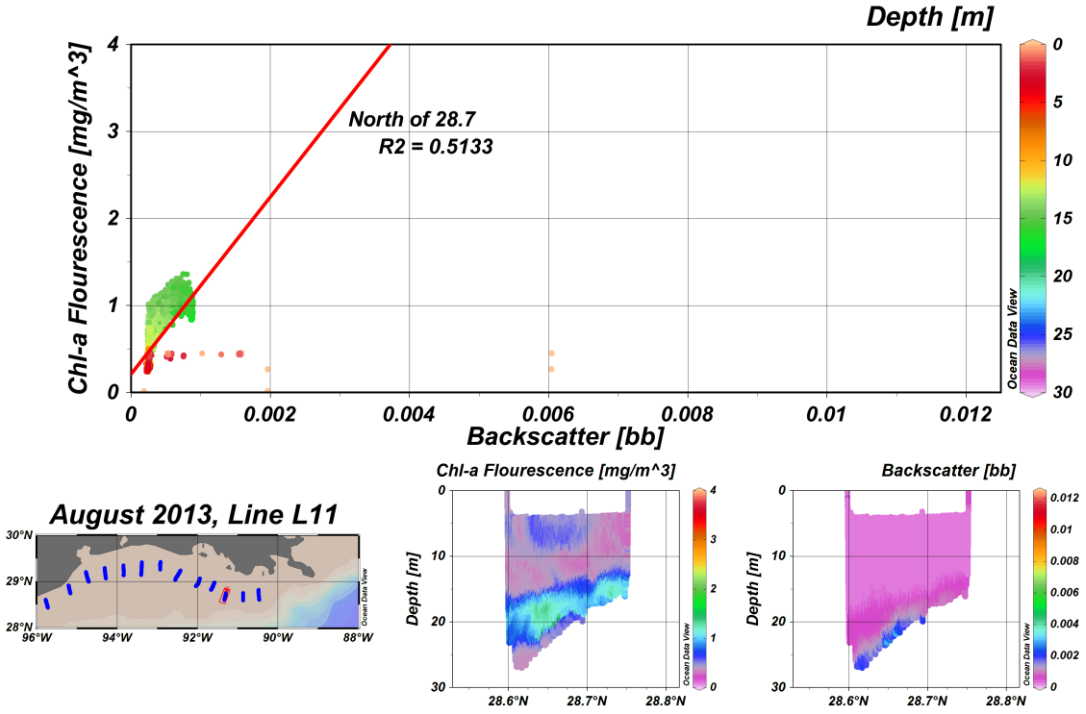

Figure 29: August 2013 Line L11 Chl-*a* Fluorescence and Backscatter, a. Landward half of Line L11 (the whole line is highlighted in red in the map), south of East Cote Blanche and Atchafalaya Bays, during August of 2013. This portion of the line (scatter plot) displays high sub-pycnocline chlorophyll-*a* flourescence corresponding with high bottom turbidity measured by proxy as backscatter. The sections display the line as a whole; the northern end displays a correlation between the chlorophyll and turbidity maximums, however the chlorophyll maximum is above the turbidity maximum on the southern end of the line. The turbidity maximum here may be due to resuspension of sediments in addition to chloropyhll.

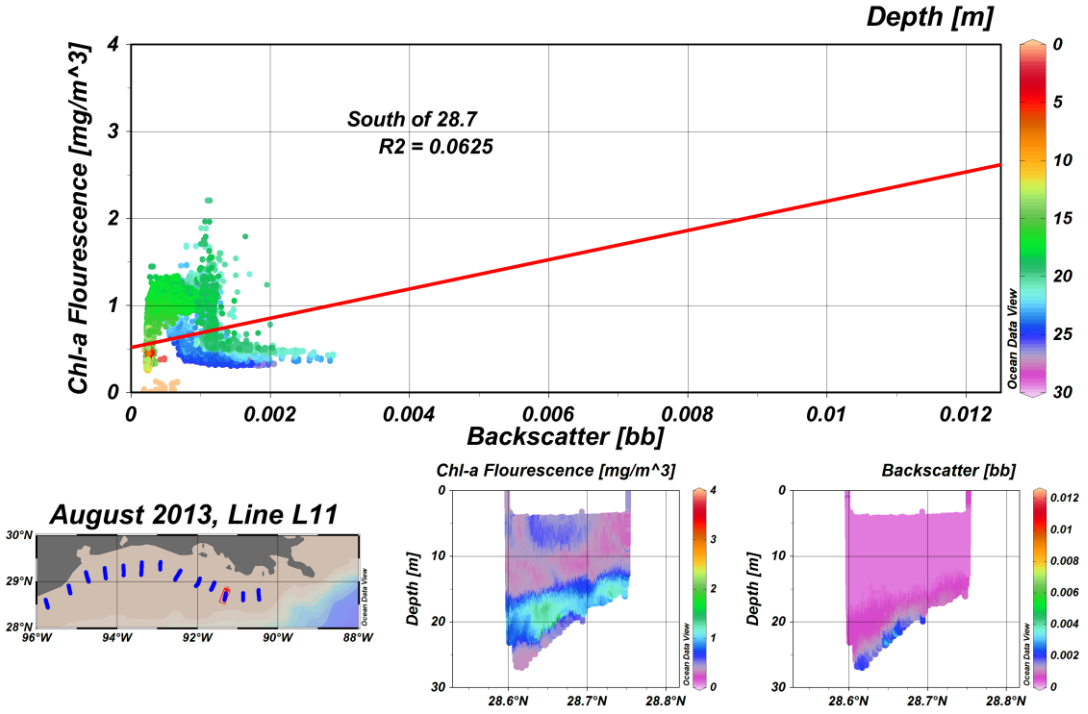

Figure 30: August 2013 Line L11 Chl-*a* Fluorescence and Backscatter, b. Seaward half of Line L11 (the whole line is highlighted in red in the map), south of East Cote Blanche and Atchafalaya Bays, during August of 2013. This portion of the line (scatter plot) displays low sub-pycnocline chlorophyll-*a* flourescence and high bottom turbidity measured by proxy as backscatter. The sections display the line as a whole; the northern end displays a correlation between the chlorophyll and turbidity maximums, however the chlorophyll maximum is above the turbidity maximum on the southern end of the line. The turbidity maximum here is likely due to resuspension of sediments.

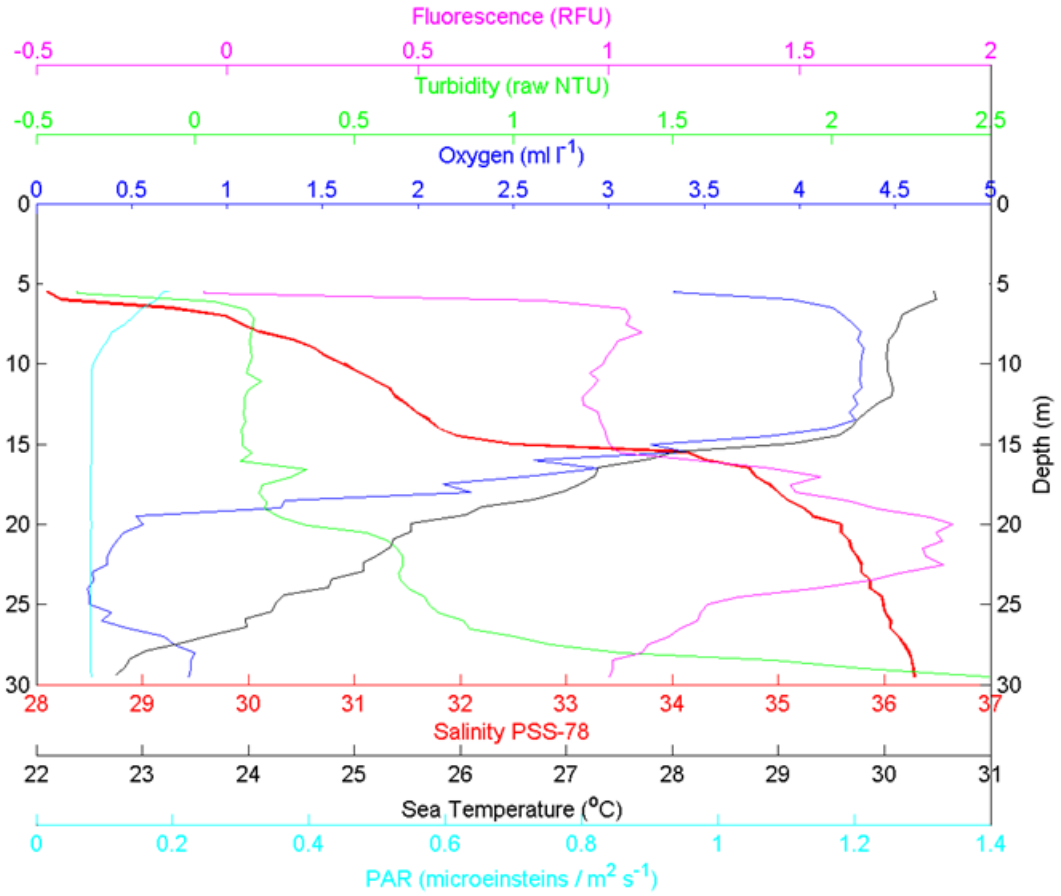

Figure 31: Chlorophyll and Turbidity Maximum Profile. August 2013 CTD cast L112, on the seaward end of Line L11 (Figure 24). Here it can be seen that although turbidity (green line) does increase at the chlorophyll fluorescence (magenta line) maximum, the turbidity maximum is below the chlorophyll maximum, therefore the turbidity in this location is likely due to resuspension of sediments. It is also interesting to note that the dissolved oxygen concentration (blue line) decreases rapidly at the high fluorescence depth, indicating that net respiration is higher than net production as inferred from chlorophyll-*a* fluorescence.

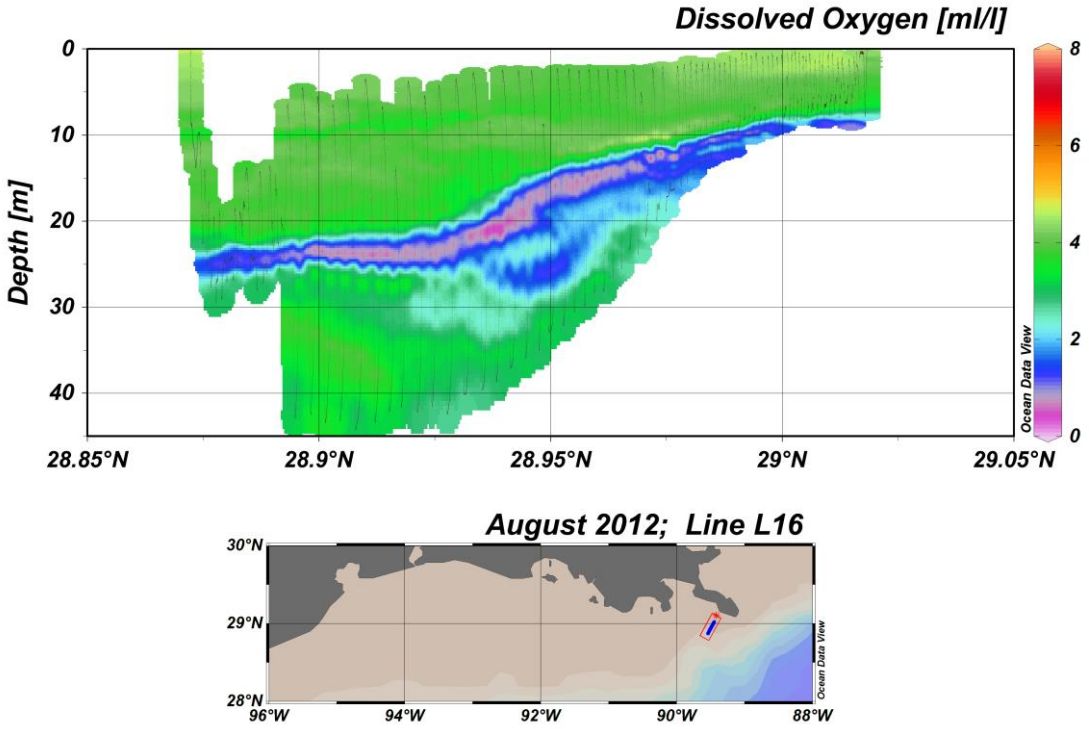

Figure 32: August 2012 Low Oxygen Feature at Line L16. Hypoxic waters extend offshore from the shallow waters near the delta. The fine black dots in the section represent each data point as the Acrobat was towed.

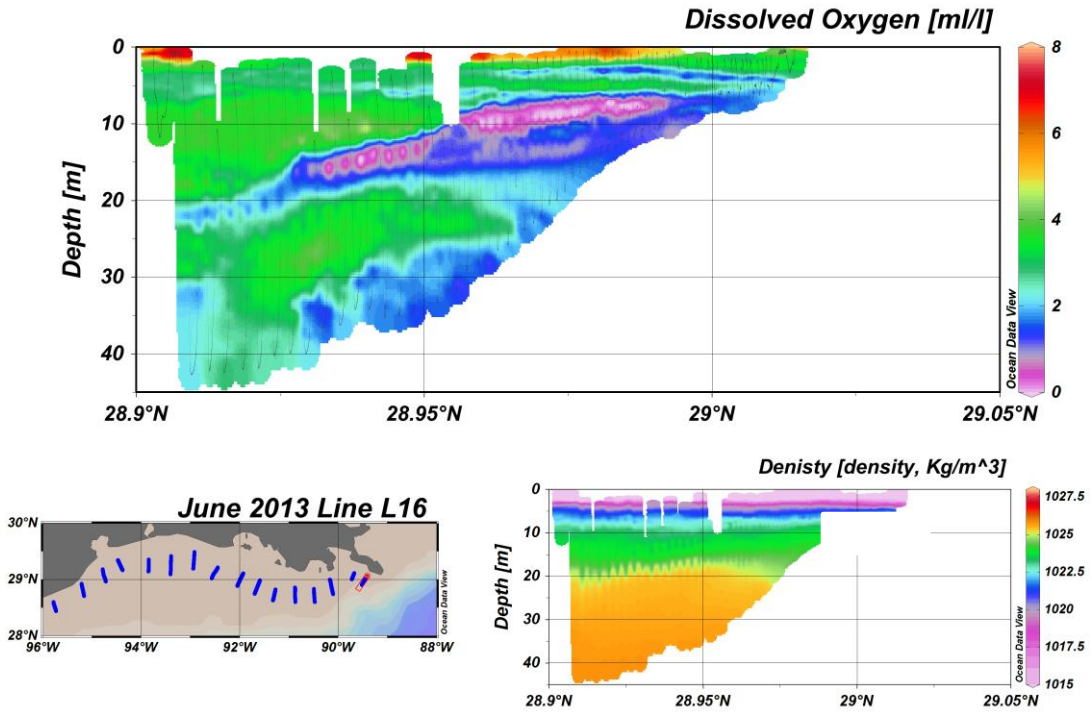

Figure 33: June 2013 Low Oxygen Feature at Line L16. Hypoxic waters extend offshore from the shallow waters near the delta (top). Similar to August 2012 (Figure 26), the hypoxic feature extends laterally from the shallows. The mid-water hypoxia may be constrained by a density gradient (bottom right). The fine black dots in the section represent each data point as the Acrobat was towed.

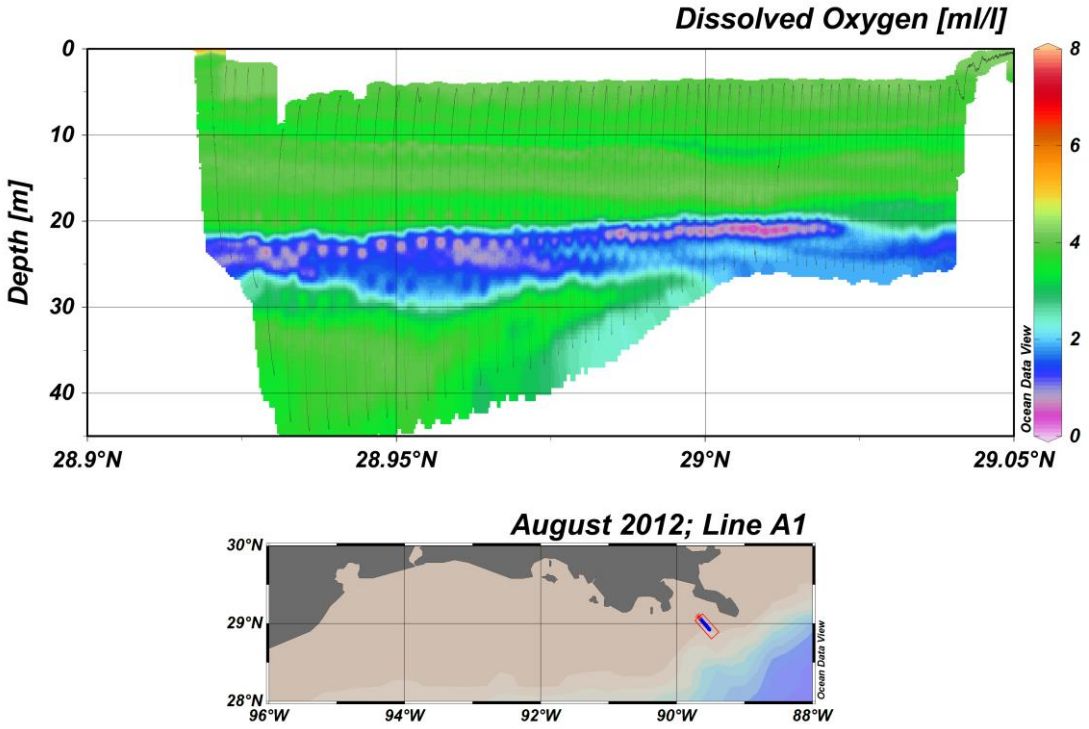

Figure 34: August 2012 Low Oxygen Feature at Line A1. Hypoxic waters extend offshore from the shallow waters near the delta. The fine black dots in the section represent each data point as the Acrobat was towed.

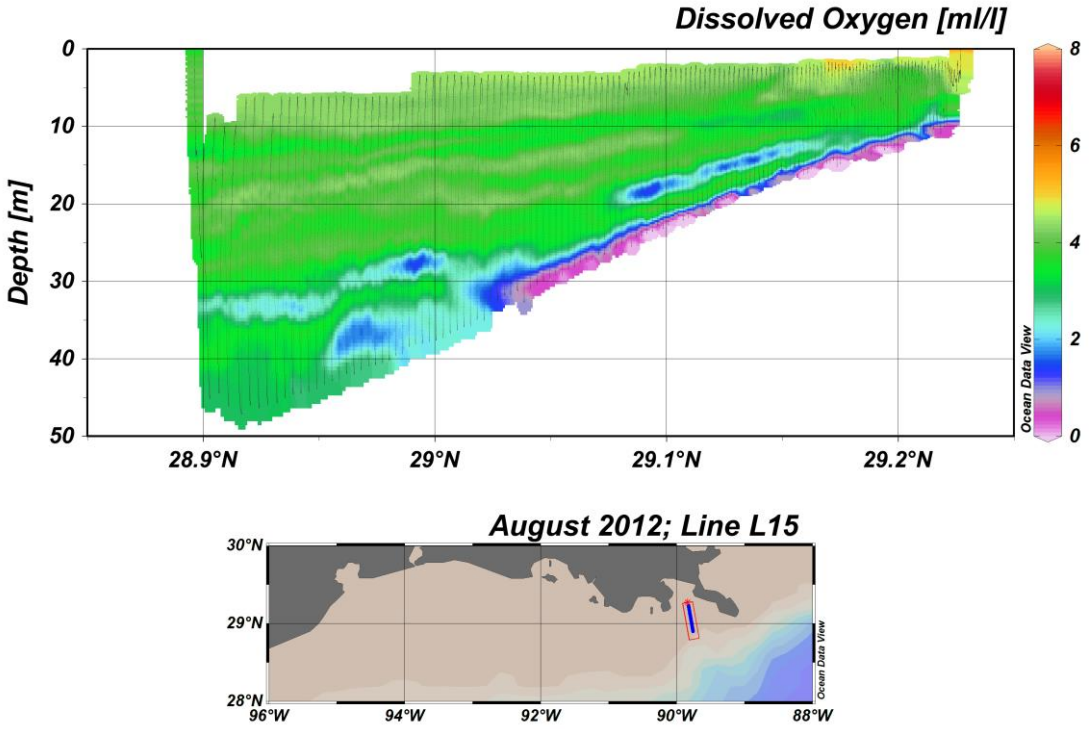

Figure 35: August 2012 Low Oxygen Feature at Line L15. Hypoxic waters extend along the bottoms from the shallow waters near the delta. This line is over a more constant topographic gradient than Line L16 (Figure 26) and Line A1 (Figure 28). The fine black dots in the section represent each data point as the Acrobat was towed.

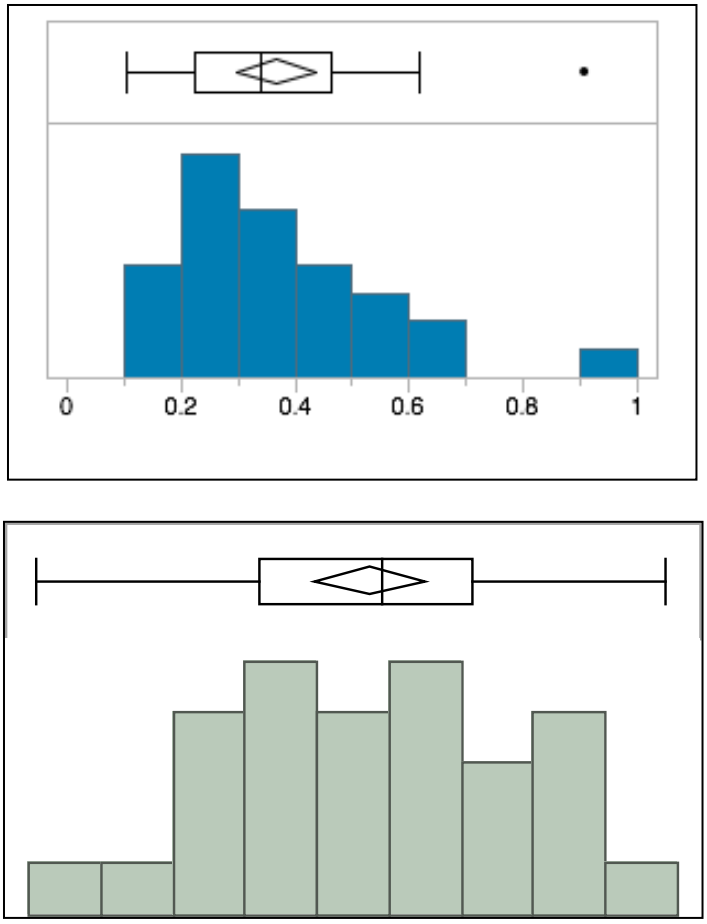

Figure 36: Histogram of Data and Transformed Data Using June 2012 POC Samples. Example of original skewed data and transformed data using June 2012 POC samples. The top histogram and box and whisker plot displays the original skewed data. Dot indicates an outlier. The bottom plots display the transformed data (ln(POC*10).

For each box and whisker plot, the vertical line within the box represents the median sample value. The confidence diamond contains the mean and the upper and lower 95% of the mean. The ends of the box represent the 1st and 3rd quartile, respectively. The whiskers extend from the ends of the box to the outermost data point (not including data deemed to be outliers).

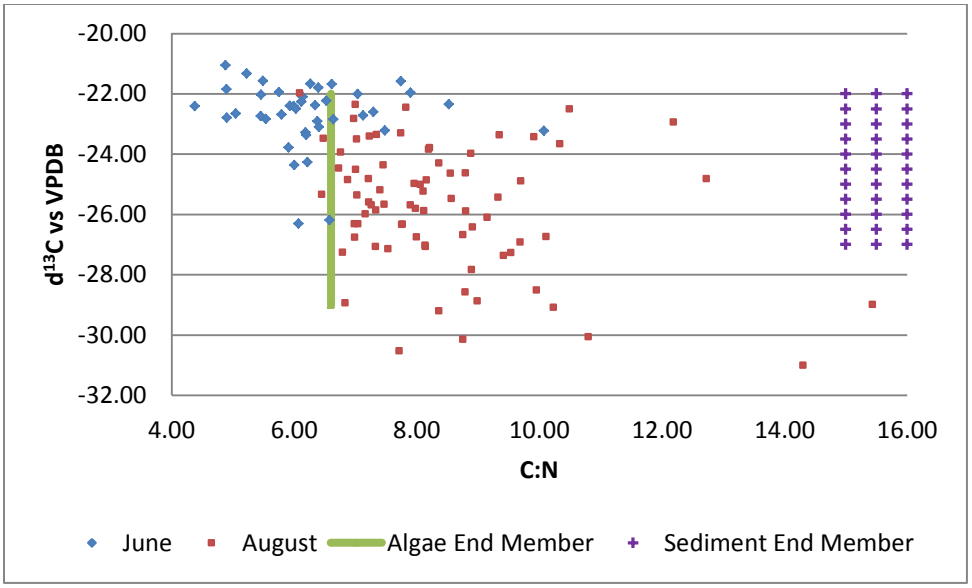

Figure 37: Stable Carbon and Nitrogen Isotope Data Collected During June 2011 and August 2011. There is a distinct depletion in ^{13}C and an increase in the ^{13}C:^{15}N ratio between June 2011 (blue) and August 2011 (red). The green line represents the algae end member (^{13}C:^{15}N = 6.6) determined from the Redfield Ratio, and the purple region represents the estuarine sediment end member [*Wissel et al.*, 2005].

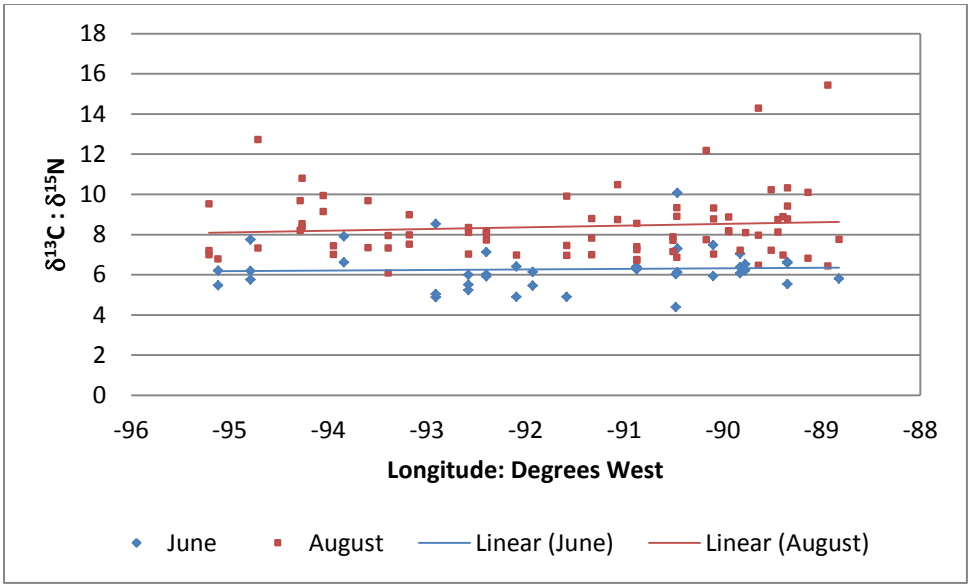

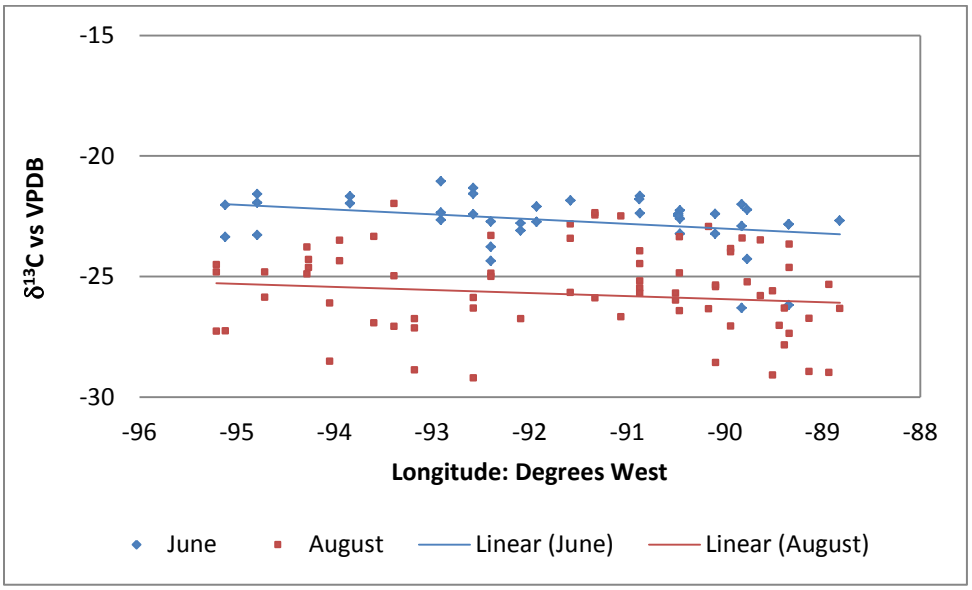

Figure 38: Stable Carbon and Nitrogen Isotope Trends with Longitude. Isotopic C:N ratio (top) and $\delta^{13}C$ (bottom) plotted as a function of longitude. These data show a distinct negative shift in $\delta^{13}C$ values from June 2011 to August 2011, as well as an increase in the ^{13}C:^{15}N ratio.

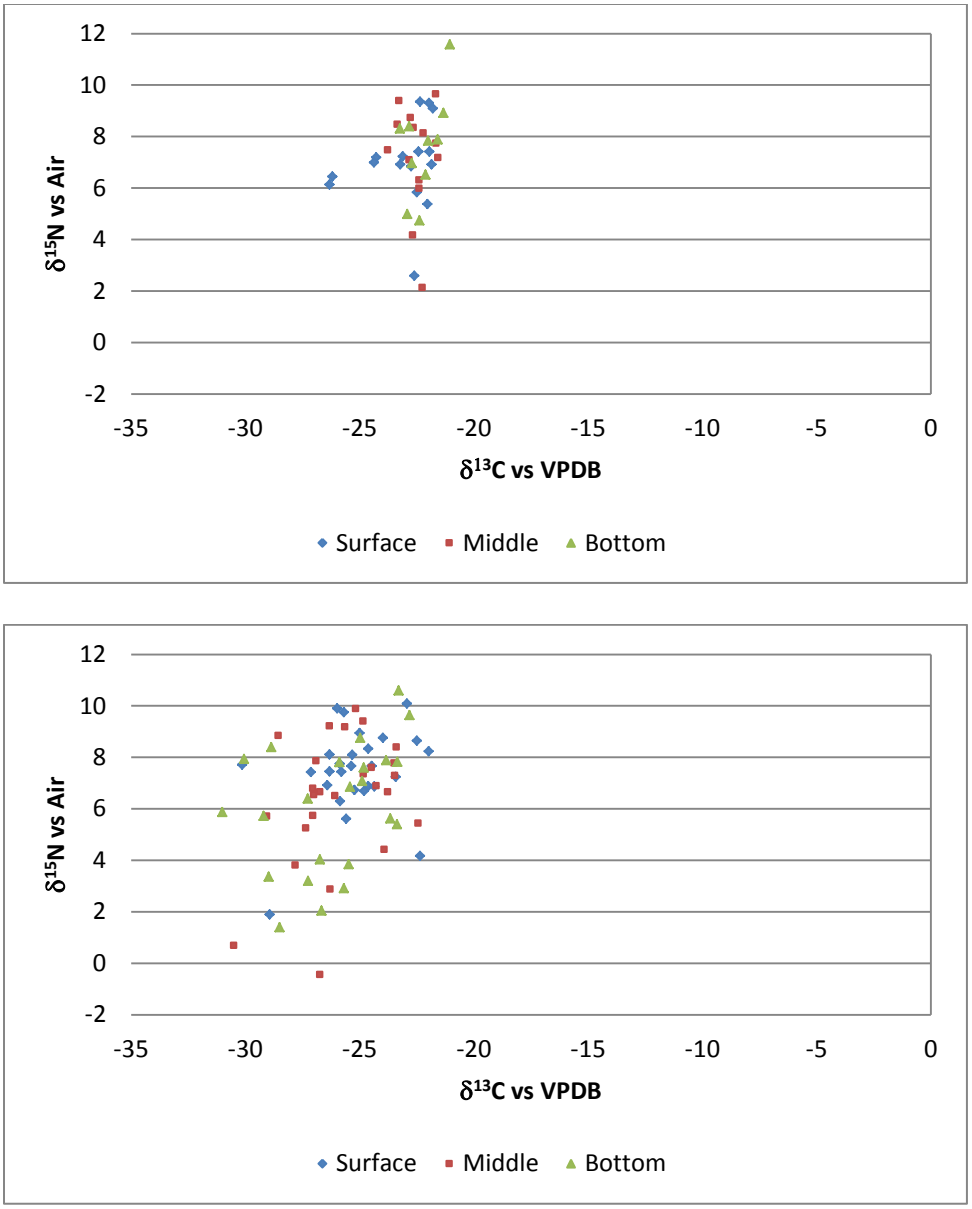

Figure 39: Stable Carbon and Nitrogen Isotope Data by Nominal Depth. Carbon and nitrogen isotope data from June 2011 (top) and August 2011 (bottom). The data do not appear significantly different between surface, middle, and bottom sample depths.

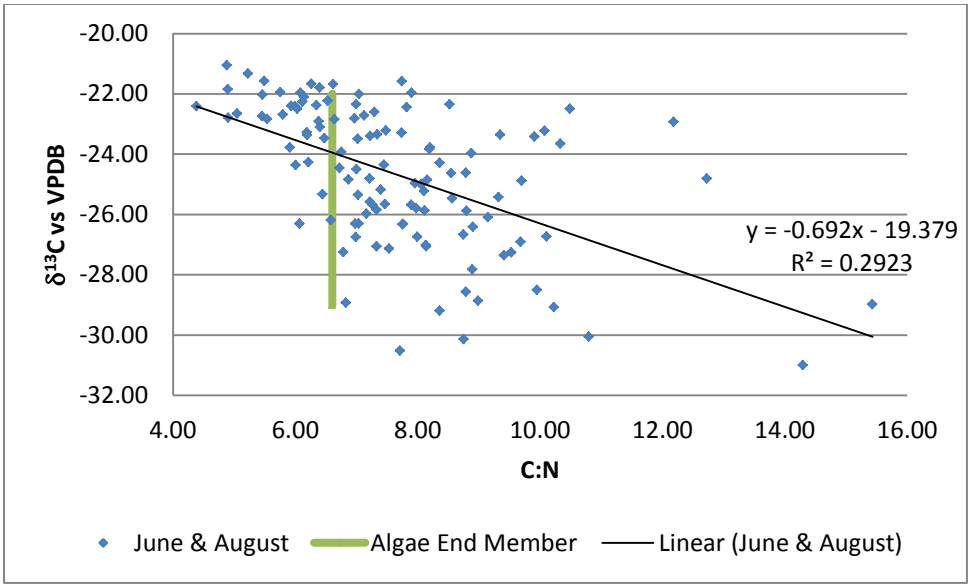

Figure 40: Stable Carbon and Nitrogen Isotope Data General Trend. Data from June 2011 and August 2011 displays a general trend of decreasing ^{13}C corresponding with an increasing C:N ratio.

APPENDIX B

TABLES

Flow-Through System in Shipboard Laboratory	**CTD**	**Acrobat**
Beam c_p WetLabs Transmissometer PM Proxy	Backscatter: 700nm WetLabs FLNTU[1] (deep) PM Proxy	Backscatter: 700nm WetLabs FLNTU (shallow) PM Proxy
Chlorophyll *a* fluorescence Chelsea Aquatracker III (2012 cruises only)	Chlorophyll *a* fluorescence WetLabs ECO FLNTU (deep) 470/695nm	Chlorophyll *a* fluorescence WetLabs ECO FLNTU (shallow) 470/695nm
CDOM fluorescence WetLabs ECO CDOM[2] 370/460nm		CDOM fluorescence WetLabs ECO CDOM 370/460nm
Salinity	Salinity	Salinity
Temperature	Temperature	Temperature
	Dissolved O_2	Dissolved O_2
	PAR	
Discrete Samples for Lab Analysis		
	Dissolved O_2	
	Nutrients	
	Particulate Matter	
	POC	

Table 1: Instruments Used to Collect Measurements During the Four Cruises. The three methods of sampling are onboard flow-through in shipboard laboratory (near surface measurements), CTD casts (bottle samples taken at discrete depths, nominally top, middle, and bottom water depths of the specific stations) , and Acrobat tows (measurements from ~1m below the surface to ~1m above the seafloor). There are no onboard flow-through data for transmissivity, chlorophyll *a* fluorescence, or CDOM fluorescence during August 2013 due to problems with the data logger.

[1] FLNTU: Chlorophyll *a* fluorometer with an optical scattering measurement at 700 nm for simultaneous determination of turbidity.
[2] ECO CDOM: Fluorometer measuring colored dissolved organic matter (CDOM).

Time Period	Average Discharge
May 2012	424,940
June 2012	244,144
July 2012	177,423
August 2012	151,788
May 2013	895,299
June 2013	858,624
July 2013	657,554
August 2013	404,241

Table 2: 2012-2013 Average Monthly Discharge May through August. The discharge values, in cubic feet per second, at the Baton Rouge, LA, gauge station clearly show the low discharge of the Mississippi following the extensive drought in its watershed in 2012 and the return to "normal" discharge in 2013 (Figure 9) [*USGS*, 2014]. This table displays the average discharge for each month during the study period.

Time Period	Average Discharge
Spring (May & June) 2012	334,542
Summer (July & August) 2012	164,605
Spring (May & June) 2013	876,961
Summer (July & August) 2013	530,898
	% Change
Spring-Summer 2012	50.8% Decrease
Spring-Summer 2013	39.5% Decrease
Spring 2012-2013	61.9% Increase
Summer 2012-2013	69.0% Increase

Table 3: 2012-2013 Average Seasonal Discharge and Inter-annual Change. The discharge values, in cubic feet per second, at the Baton Rouge, LA, gauge station clearly show the low discharge of the Mississippi following the extensive drought in its watershed in 2012 and the return to "normal" discharge (note percent increases) in 2013 (Figure 9) [*USGS*, 2014]. This table displays the seasonal averages (top) and the magnitude of change between years and seasons (bottom). Spring averages include May and June data for their respective years, and summer averages include July and August data.

Time Period	Nominal Depth	Variable	Alternative Hypothesis	P-Value	Decision
June-August 2012	T	PM	Ha: A > B	0.3687	Do Not Reject
June-August 2012	M	PM		0.7190	Do Not Reject
June-August 2012	B	PM		0.2016	Do Not Reject
June-August 2013	T	PM	Ha: A > B	0.0021	**Reject**
June-August 2013	M	PM		0.3532	Do Not Reject
June-August 2013	B	PM		0.0008	**Reject**
June 2012-2013	T	PM	Ha: A < B	0.0003	**Reject**
June 2012-2013	M	PM		0.1126	Do Not Reject
June 2012-2013	B	PM		0.0167	**Reject**
August 2012-2013	T	PM	Ha: A < B	0.0903	Do Not Reject
August 2012-2013	M	PM		0.1389	Do Not Reject
August 2012-2013	B	PM		0.6582	Do Not Reject
Time Period	**Nominal Depth**	**Variable**	**Alternative Hypothesis**	**P-Value**	**Decision**
June-August 2012	T	%POC	Ha: A > B	0.1095	Do Not Reject
June-August 2012	M	%POC		0.0039	**Reject**
June-August 2012	B	%POC		0.1934	Do Not Reject
June-August 2013	T	%POC	Ha: A > B	0.4763	Do Not Reject
June-August 2013	M	%POC		0.2750	Do Not Reject
June-August 2013	B	%POC		0.9831	Do Not Reject
June 2012-2013	T	%POC	Ha: A < B	0.9452	Do Not Reject
June 2012-2013	M	%POC		0.9952	Do Not Reject
June 2012-2013	B	%POC		0.9994	Do Not Reject
August 2012-2013	T	%POC	Ha: A < B	0.4819	Do Not Reject
August 2012-2013	M	%POC		0.3571	Do Not Reject
August 2012-2013	B	%POC		0.5343	Do Not Reject

Table 4a: H1 Wilcoxin Summary for PM and %POC. Summary of the Wilcoxin Rank-Sum test results for inter-annual and seasonal changes in PM and %POC. A decision of "reject" indicates that the null hypothesis (both data sets display no statistical difference) should be rejected.

Time Period	Nominal Depth	Variable	Alternative Hypothesis	P-Value	Decision
June-August 2012	T	POC	Ha: A > B	0.0038	**Reject**
June-August 2012	M	POC		0.0002	**Reject**
June-August 2012	B	POC		0.0069	**Reject**
June-August 2013	T	POC	Ha: A > B	0.0001	**Reject**
June-August 2013	M	POC		0.2683	Do Not Reject
June-August 2013	B	POC		0.1296	Do Not Reject
June 2012-2013	T	POC	Ha: A < B	0.0000	**Reject**
June 2012-2013	M	POC		0.9414	Do Not Reject
June 2012-2013	B	POC		0.9748	Do Not Reject
August 2012-2013	T	POC	Ha: A < B	0.0374	**Reject**
August 2012-2013	M	POC		0.0434	**Reject**
August 2012-2013	B	POC		0.8397	Do Not Reject
Time Period	**Nominal Depth**	**Variable**	**Alternative Hypothesis**	**P-Value**	**Decision**
June-August 2012	T	C:N	Ha: A < B	0.2937	Do Not Reject
June-August 2012	M	C:N		0.0004	**Reject**
June-August 2012	B	C:N		0.0120	**Reject**
June-August 2013	T	C:N	Ha: A < B	0.0002	**Reject**
June-August 2013	M	C:N		0.0004	**Reject**
June-August 2013	B	C:N		0.0317	**Reject**
June 2012-2013	T	C:N	Ha: A > B	0.0000	**Reject**
June 2012-2013	M	C:N		0.0019	**Reject**
June 2012-2013	B	C:N		0.0097	**Reject**
August 2012-2013	T	C:N	Ha: A > B	0.1761	Do Not Reject
August 2012-2013	M	C:N		0.0003	**Reject**
August 2012-2013	B	C:N		0.0039	**Reject**

Table 4b: H1 Wilcoxin Summary for POC and C:N. Summary of the Wilcoxin Rank-Sum test results for inter-annual and seasonal changes in POC and C:N. A decision of "reject" indicates that the null hypothesis should be rejected.

Bottle Data						Acrobat Data					
Cruise	**Variable**	**Nominal Depth**	**N**	**Slope**	**R^2**	**Cruise**	**Variable**	**Longitude Range**	**N**	**Slope**	**R^2**
June 2012	PM	M	3	Positive	**0.9984**	June 2012	b_b	All Lines	10564	Negative	0.0019
June 2012	PM	B	11	Positive	0.0829	June 2012	b_b	88-90	10559	Negative	0.0020
June 2012	POC	M	3	Positive	0.0558	June 2012	b_b	90-92	0	-	-
June 2012	POC	B	11	Negative	0.1973	June 2012	b_b	92-94	0	-	-
						June 2012	b_b	94-96	0	-	-
August 2012	PM	M	3	Positive	0.2764	August 2012	b_b	All Lines	37077	Negative	0.0002
August 2012	PM	B	9	Positive	0.5972	August 2012	b_b	88-90	21622	Negative	0.0006
August 2012	POC	M	3	Positive	**0.9987**	August 2012	b_b	90-92	15455	Negative	0.0008
August 2012	POC	B	9	Positive	0.0286	August 2012	b_b	92-94	0	-	-
						August 2012	b_b	94-96	0	-	-
June 2013	PM	M	3	Positive	0.1333	June 2013	b_b	All Lines	154656	Positive	0.0108
June 2013	PM	B	17	Positive	0.0637	June 2013	b_b	88-90	14212	Positive	0.0014
June 2013	POC	M	3	Negative	0.0002	June 2013	b_b	90-92	75509	Positive	0.0058
June 2013	POC	B	17	Negative	0.0429	June 2013	b_b	92-94	62025	Positive	0.0149
						June 2013	b_b	94-96	6641	Positive	0.0067
August 2013	PM	M	8	Positive	0.3983	August 2013	b_b	All Lines	85256	Negative	0.0040
August 2013	PM	B	22	Positive	0.0728	August 2013	b_b	88-90	0	-	-
August 2013	POC	M	8	Negative	0.0453	August 2013	b_b	90-92	68629	Negative	0.0458
August 2013	POC	B	22	Positive	0.029	August 2013	b_b	92-94	15802	Positive	0.2485
						August 2013	b_b	94-96	0	-	-

Table 5: Summary of Bottle Data and Acrobat Data. Data displays the correlations between low oxygen (concentration < 2ml/l) and PM, POC, or b_b. There are not enough data points to observe the bottle data spatially along shelf, thus this data are sorted by the nominal sample depths. The Acrobat data only uses data collected from below 2m water depth, as surface water is well oxygenated. The two bold values indicate strong, positive correlations.

Cruise	Longitude Range	Variables	N	R^2	Variables	N	R^2	Variables	N	R^2
June 2012	All	**b_b-O_2**	10190	0.0297	**b_b-chl**	9981	0.0487	**chl-O_2**	10190	0.0005
June 2012	88-90	**b_b-O_2**	10190	0.0297	**b_b-chl**	9981	0.0487	**chl-O_2**	10190	0.0005
June 2012	90-92	**b_b-O_2**	0	-	**b_b-chl**	0	-	**chl-O_2**	0	-
June 2012	92-94	**bb-O_2**	0	-	**b_b-chl**	0	-	**chl-O_2**	0	-
June 2012	94-96	**b_b-O_2**	0	-	**b_b-chl**	0	-	**chl-O_2**	0	-
August 2012	All	**b_b-O_2**	36013	0.0004	**b_b-chl**	34742	0.1283	**chl-O_2**	36013	0.0143
August 2012	88-90	**b_b-O_2**	21075	0.0005	**b_b-chl**	20472	0.0552	**chl-O_2**	21075	0.1499
August 2012	90-92	**b_b-O_2**	14938	0.0287	**b_b-chl**	14270	0.0491	**chl-O_2**	14938	0.0487
August 2012	92-94	**b_b-O_2**	0	-	**b_b-chl**	0	-	**chl-O_2**	0	-
August 2012	94-96	**b_b-O_2**	0	-	**b_b-chl**	0	-	**chl-O_2**	0	-
June 2013	All	**b_b-O_2**	135736	0.0180	**b_b-chl**	131990	0.0006	**chl-O_2**	135741	0.0062
June 2013	88-90	**b_b-O_2**	11129	0.0004	**b_b-chl**	10801	0.4230	**chl-O_2**	11129	0.0087
June 2013	90-92	**b_b-O_2**	60378	0.0096	**b_b-chl**	56889	0.1218	**chl-O_2**	58863	0.0013
June 2013	92-94	**b_b-O_2**	59116	0.0184	**b_b-chl**	56668	0.0083	**chl-O_2**	57538	0.0061
June 2013	94-96	**b_b-O_2**	6632	0.0048	**b_b-chl**	6076	0.0453	**chl-O_2**	6632	0.0084
August 2013	All	**b_b-O_2**	77598	0.0002	**b_b-chl**	75622	0.2008	**chl-O_2**	77598	0.1112
August 2013	88-90	**b_b-O_2**	No data	No data	**b_b-chl**	No data	No data	**chl-O_2**	No data	No data
August 2013	90-92	**b_b-O_2**	58077	0.0245	**b_b-chl**	59130	0.0563	**chl-O_2**	59365	0.1266
August 2013	92-94	**b_b-O_2**	17836	0.2089	**b_b-chl**	17458	0.2660	**chl-O_2**	18172	0.0931
August 2013	94-96	**b_b-O_2**	0	-	**b_b-chl**	0	-	**chl-O_2**	0	-

Table 6: Correlations by Longitude Zone. Data greater than 10m water depth to seafloor for hypoxic longitude zones. Variables are backscatter (b_b), dissolved oxygen (O_2), and chlorophyll-*a* fluorescence (chl). When N = 0, it indicates that zone was surveyed, but was not experiencing hypoxic conditions at the time surveyed. There are no Acrobat data in the 88°-90° W during August 2013.

Cruise	Line	Variables	N	R^2	Variables	N	R^2	Variables	N	R^2
June 2012	L16	**b_b-O_2**	21490	0.1086	**b_b-chl**	21490	0.0143	**chl-O_2**	21490	0.1691
June 2012	L15	**b_b-O_2**	56395	0.0784	**b_b-chl**	56395	0.0265	**chl-O_2**	56395	0.2316
August 2012	L16, A1	**b_b-O_2**	60433	0.0169	**b_b-chl**	60446	0.1895	**chl-O_2**	60433	0.1170
August 2012	L15, A2	**b_b-O_2**	107883	0.1257	**b_b-chl**	108059	0.0261	**chl-O_2**	107883	0.1848
August 2012	L14	**b_b-O_2**	48143	0.2436	**b_b-chl**	48261	0.1861	**chl-O_2**	48143	0.3237
August 2012	L13	**b_b-O_2**	44167	0.0205	**b_b-chl**	44167	0.1996	**chl-O_2**	44167	0.1502
August 2012	L11	**b_b-O_2**	24933	0.0775	**b_b-chl**	24933	0.3213	**chl-O_2**	24933	0.0223
August 2012	L10	**b_b-O_2**	42377	0.2746	**b_b-chl**	42377	**0.4417**	**chl-O_2**	42377	**0.6879**
June 2013	L16	**b_b-O_2**	23512	0.3106	**b_b-chl**	23684	0.2241	**chl-O_2**	23514	0.3330
June 2013	L15	**b_b-O_2**	22130	0.0076	**b_b-chl**	22145	0.2407	**chl-O_2**	22130	0.1117
June 2013	L14	**b_b-O_2**	42196	0.2560	**b_b-chl**	42197	0.0016	**chl-O_2**	42200	0.2888
June 2013	L13	**b_b-O_2**	41022	0.0013	**b_b-chl**	41234	0.3852	**chl-O_2**	41022	0.1514
June 2013	L12	**b_b-O_2**	47114	0.0033	**b_b-chl**	48262	0.0503	**chl-O_2**	47118	0.2448
June 2013	L11	**b_b-O_2**	35301	0.0910	**b_b-chl**	36291	0.0002	**chl-O_2**	35301	0.0588
June 2013	L10	**b_b-O_2**	44063	0.2877	**b_b-chl**	44111	0.0007	**chl-O_2**	44063	0.0382
June 2013	L9	**b_b-O_2**	43781	0.2345	**b_b-chl**	43864	0.0523	**chl-O_2**	43783	0.1333
June 2013	L8	**b_b-O_2**	38844	**0.4577**	**b_b-chl**	39511	0.1323	**chl-O_2**	38844	0.0100
June 2013	L7	**b_b-O_2**	50715	0.2463	**b_b-chl**	51418	0.0184	**chl-O_2**	50715	0.0002
June 2013	L6	**b_b-O_2**	56627	**0.4692**	**b_b-chl**	56796	0.0062	**chl-O_2**	56627	0.0514
June 2013	L5	**b_b-O_2**	36262	0.2012	**b_b-chl**	36262	0.0347	**chl-O_2**	36263	0.0902
June 2013	L4	**b_b-O_2**	33476	0.3201	**b_b-chl**	33476	**0.6106**	**chl-O_2**	33476	**0.5304**
June 2013	L3	**b_b-O_2**	37983	**0.6727**	**b_b-chl**	37983	0.2279	**chl-O_2**	37985	0.2299
June 2013	L2	**b_b-O_2**	39005	**0.7007**	**b_b-chl**	39005	0.3944	**chl-O_2**	39005	0.2755
June 2013	L1	**b_b-O_2**	28507	**0.5643**	**b_b-chl**	28507	0.4378	**chl-O_2**	28507	**0.6641**
August 2013	L13	**b_b-O_2**	35688	0.0384	**b_b-chl**	37021	**0.4418**	**chl-O_2**	35688	0.4975
August 2013	L12	**b_b-O_2**	28089	0.0208	**b_b-chl**	28925	0.2949	**chl-O_2**	28089	0.3707
August 2013	L11	**b_b-O_2**	27771	**0.5619**	**b_b-chl**	27950	0.1176	**chl-O_2**	27771	**0.5444**
August 2013	L10	**b_b-O_2**	31750	0.3567	**b_b-chl**	31770	0.1190	**chl-O_2**	31750	0.0925
August 2013	L9	**b_b-O_2**	33119	0.3461	**b_b-chl**	34049	0.0446	**chl-O_2**	33119	0.0003
August 2013	L8	**b_b-O_2**	42364	0.3585	**b_b-chl**	43071	0.3672	**chl-O_2**	42364	0.1900
August 2013	L7	**b_b-O_2**	31213	0.2393	**b_b-chl**	31249	0.2088	**chl-O_2**	31213	**0.4301**
August 2013	L6	**b_b-O_2**	50241	**0.4030**	**b_b-chl**	50244	0.2611	**chl-O_2**	50241	0.3932
August 2013	L5	**b_b-O_2**	38849	0.3257	**b_b-chl**	38849	0.0241	**chl-O_2**	38849	0.0356

Table 7: Correlations in Individual Acrobat Lines. This table displays data from Acrobat lines that experienced hypoxic conditions at the time surveyed. Variables are backscatter (b_b), dissolved oxygen (O_2), and chlorophyll-*a* fluorescence (chl). Moderate to strong R^2 correlations between variable sets have been made bold, and lines are organized from east to west for each cruise. The strongest correlations occur toward the western end of the shelf.

Time Period	Nominal Depth	Variable	Alternative Hypothesis	P-Value	Decision
June 2011 - August 2011	N/A	^{15}N	Ha: A < B	0.7553	Do Not Reject
June 2011 - August 2011	N/A	^{15}N	Ha: A > B	0.2447	Do Not Reject
June 2011 - August 2011	N/A	^{13}C	Ha: A > B	1.679E-13	**Reject**
June 2011 - August 2011	N/A	^{13}C:^{15}N	Ha: A < B	1.730E-14	**Reject**

Table 8: H4 Wilcoxin Summary. Wilcoxin Rank-Sum test results for the June 2011 and August 2011 isotope data. The ^{15}N is statically the same between cruises, ^{13}C is statically higher in June, and the C:N ratio is statically lower in June.